

Electronic Supporting Information

**[(TMEDA)Li(μ -PPh₂)₂K(TMEDA)(THF)]: a heterobimetallic
molecular lithium-potassium phosphide complex**

Michelle H. Crabbe, Danielle O'Meara, Alan R. Kennedy, Catherine E. Weetman and Robert E. Mulvey

Department of Pure and Applied Chemistry, University of Strathclyde, Glasgow, G1 1XL, UK
E-mail: catherine.weetman@strath.ac.uk and r.e.mulvey@strath.ac.uk

Table of Contents

1. Experimental	2
1.1 General Methods and Instruments	2
1.2 Synthesis and Characterisation	3
KPPh ₂	3
[(TMEDA)Li(μ -PPh ₂) ₂ K(TMEDA)(THF)] (1) – toluene-d ₈	5
[(TMEDA)Li(μ -PPh ₂) ₂ K(TMEDA)(THF)] (1) – benzene-d ₆	9
¹ H DOSY NMR for [(TMEDA)Li(μ -PPh ₂) ₂ K(TMEDA)(THF)] (1) – toluene-d ₈	12
[LiPPh ₂ (TMEDA)] ₂ – toluene-d ₈ and THF	14
[KPPh ₂ (TMEDA)] _n – toluene-d ₈ and THF	16
2. Single Crystal X-Ray Crystallography (SC-XRD)	20
2.1 General Crystallographic Information	20
2.2 Selected Bond Lengths and Angles	21
2.3 Low Hapticity Analysis	22
3. Catalytic Hydrophosphination	23
3.1 Hydrophosphination of 1,1-DPE Using 1	23
3.2 Hydrophosphination of 1,1-DPE Using 5 mol% 1	25
3.3 Hydrophosphination of 1,1-DPE Using [LiPPh ₂ (TMEDA)] ₂	27
3.4 Hydrophosphination of 1,1-DPE Using [LiPPh ₂ (TMEDA)] ₂ and THF	29
3.5 Hydrophosphination of 1,1-DPE Using [KPPh ₂ (TMEDA)] _n	31
3.6 Hydrophosphination of 1,1-DPE Using [KPPh ₂ (TMEDA)] _n with THF	33
3.7 Hydrophosphination Dehydrocoupling Control with 1	35
4. Computational Details	36
4.1 QTAIM Analysis	37
4.2 NMR Calculations	38
4.3 Reaction Energy Profiles	39
5. References	40

1. Experimental

1.1 General Methods and Instruments

All synthetic procedures were performed under inert gas (N_2 or argon) using standard Schlenk techniques¹ or an Innovative Technology PureLab HE glovebox. Prior to use, all glassware was heated thrice under vacuum. Ground glass joints were coated with IKV Tribology high temperature fluorinated grease. Unless otherwise stated, all chemicals were purchased from Sigma-Aldrich, Fluorochem, Thermo Fisher or Alfa Aesar and used as received. THF, n-hexane and toluene were dried and dispensed by an Innovative Technology Solvent Purification System. TMEDA was dried over CaH_2 , distilled under N_2 and stored over activated 4 Å molecular sieves. All solvents including benzene- d_6 and toluene- d_8 were stored over activated 4 Å molecular sieves for a minimum of 24 h prior to use. $LiPPh_2$ ² and $KN(SiMe_3)_2$ ³ were synthesised according to literature procedures. NMR samples were prepared in an argon filled glovebox, and all NMR spectra were recorded on a Bruker AV400 spectrometer operating at 400.1 MHz (1H), 100.6 MHz (^{13}C), 162.0 MHz (^{31}P) or 155.5 MHz (7Li) and measured at 300 K. ^{13}C spectra were run 1H decoupled. Chemical shifts are reported in parts per million (δ , ppm). 1H NMR chemical shifts are referenced to residual proton resonances of the corresponding deuterated solvent. ^{13}C NMR chemical shifts are reported relative to TMS (tetramethylsilane) using the carbon resonances of the deuterated solvent. ^{31}P NMR spectra are referenced relative to 85% H_3PO_4 in D_2O . 7Li NMR spectra are referenced relative to $LiCl$ in D_2O . Signal multiplicities have been described using common abbreviations as follows: s (singlet), d (doublet), t (triplet), m (multiplet) and tt (triplet of triplets).

1.2 Synthesis and Characterisation

KPPh₂

Synthesis was based on an amended literature procedure.⁴ HPPH₂ (0.48 mL, 2.76 mmol) was dissolved in hexane (15 mL) which gave a colourless solution, then KN(SiMe₃)₂ (0.56 g, 2.80 mmol) was added. An orange precipitate formed immediately, and the mixture was stirred at room temperature for 15 minutes. The solid was isolated *via* filtration, triturated with toluene (5 mL) and hexane (2 x 5 mL) and dried under reduced pressure to give the product as an orange powder, 0.56 g, yield = 83%. An NMR sample was prepared by suspending the product in 0.5 mL toluene-d₈ and adding THF (0.06 mL).

¹H NMR (toluene-d₈, 300 K) δ_H (ppm): 7.70 (t, 2H, *H*_{Ar}, ³*J*_{HH} = 6.66 Hz); 6.95 (t, 2H, *H*_{Ar}, ³*J*_{HH} = 7.54 Hz); 6.68 (t, 1H, *H*_{Ar}, ³*J*_{HH} = 7.22 Hz).

¹³C{¹H} NMR (toluene-d₈) δ_C (ppm): 154.8 (d, *C*_{Ar}, ¹*J*_{C-P} = 45.0 Hz, 129.6 (d, *C*_{Ar}, ²*J*_{C-P} = 17.7 Hz), 128.5 (d, *C*_{Ar}, ³*J*_{C-P} = 5.28 Hz), 120.3 (*C*_{Ar}).

³¹P NMR (toluene-d₈) δ_P (ppm): -17.3.

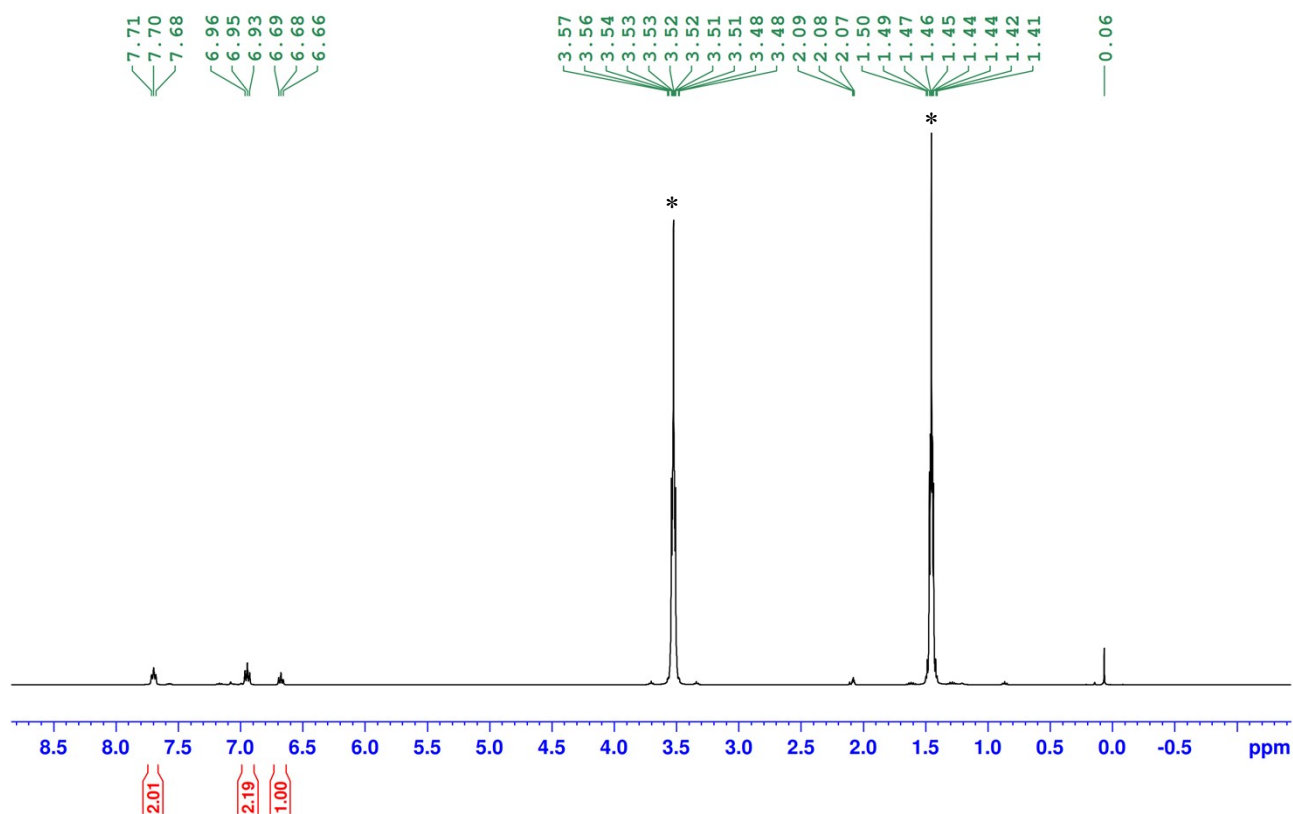


Figure S1 ¹H NMR spectrum of KPPh₂ in toluene-d₈. THF (*) and small amounts of toluene and HMDS(H) are also present.

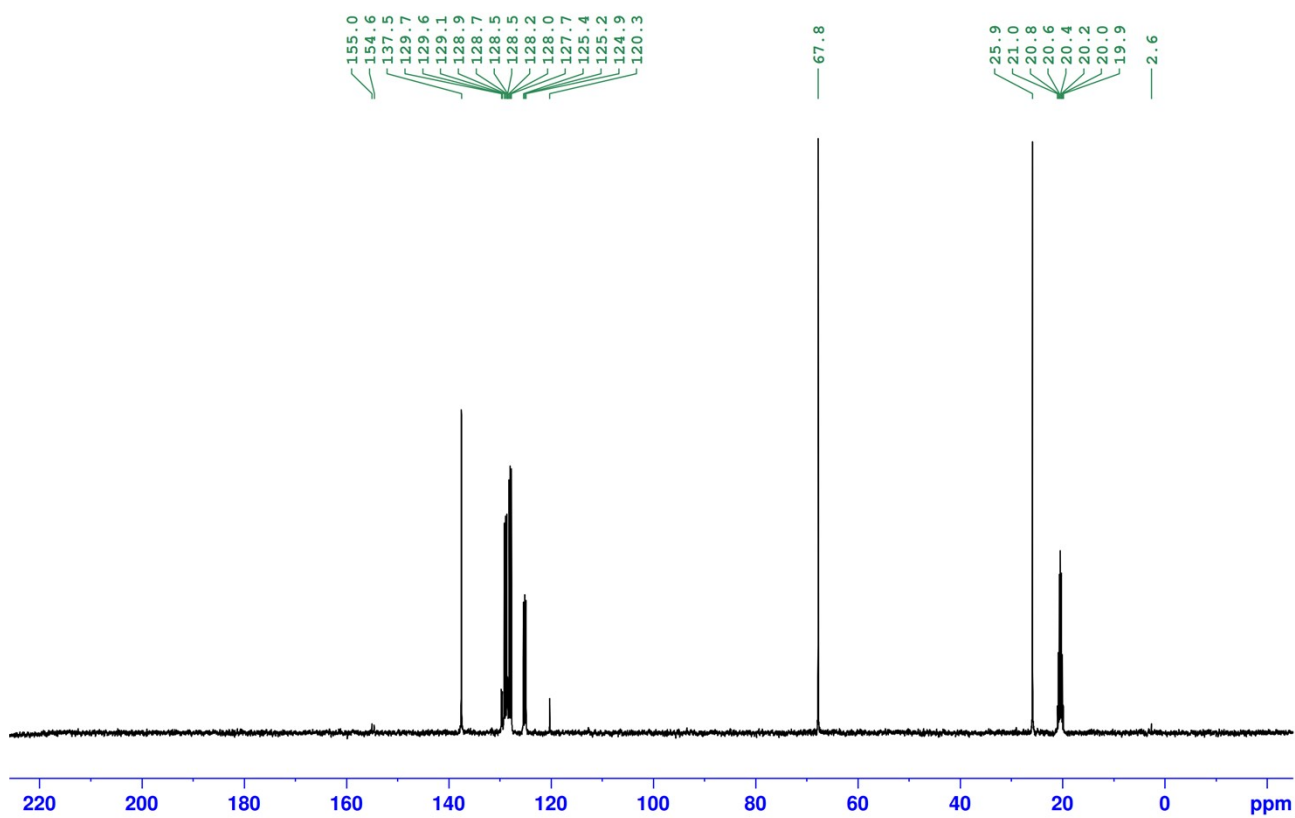


Figure S2 $^{13}\text{C}\{^1\text{H}\}$ NMR spectrum of KPh_2 in toluene- d_8 . THF (*) and a small amount of HMDS(H) are also present.

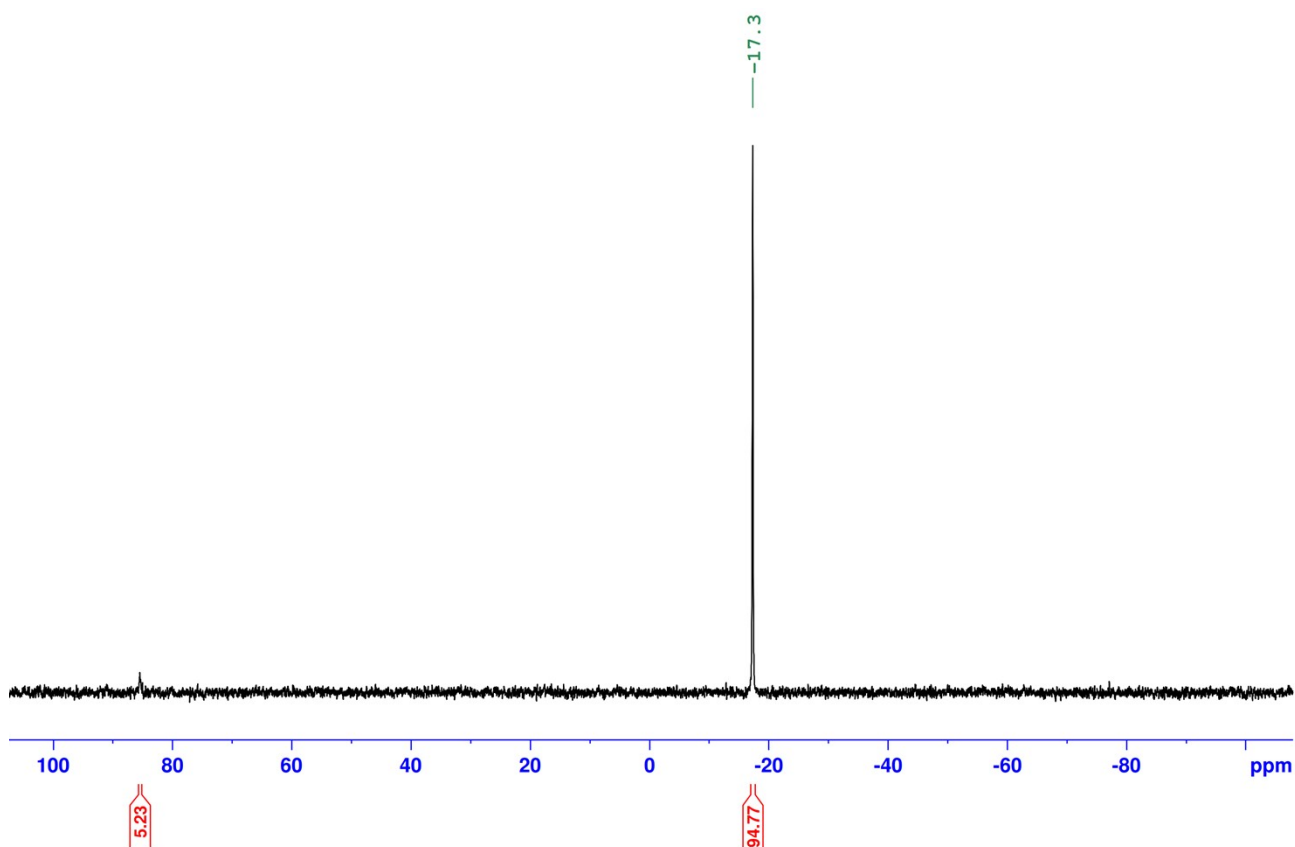


Figure S3 ^{31}P NMR spectrum of KPh_2 in toluene- d_8 . A small amount of $\text{Ph}_2\text{P}(\text{OK})$ (-85 ppm) is also present.

[(TMEDA)Li(μ -PPh₂)₂K(TMEDA)(THF)] (**1**) – toluene-d₈

LiPPh₂ (0.192 g, 1 mmol) and KPPh₂ (0.224 g, 1 mmol) were suspended in toluene (10 mL) and stirred for 1 hour. To this suspension, TMEDA (0.28 mL, 2 mmol, 2 eq.) and THF (1 mL, 12 eq.) were added. The solvent was removed from the resulting orange solution under reduced pressure to give an orange oil. Hexane (40 mL) was added and the mixture for sonicated for 1h, resulting in an orange solid and yellow supernatant. The mixture was filtered and the solid dried under reduced pressure to give the product as an orange powder, crude yield = 0.52 g, 72 %. In an attempt to grow crystals, a suspension of the orange powder in toluene and THF was heated at 110 °C for 5 minutes, and then the resulting solution was cooled at -30 °C for 48 h. From this, orange crystals suitable for X-ray crystallographic study were obtained. An NMR sample was prepared by suspending the product in 0.5 mL toluene-d₈ and adding THF (0.05 mL).

¹H NMR (toluene-d₈, 300 K) δ_{H} (ppm): 7.77 (t, 4H, H_{Ar} , $^3J_{\text{HH}} = 6.65$ Hz); 7.02 (t, 4H, H_{Ar} , $^3J_{\text{HH}} = 7.50$ Hz); 6.73 (tt, 2H, H_{Ar} , $^3J_{\text{HH}} = 1.17$ Hz, $^3J_{\text{HH}} = 7.22$ Hz); 2.11 (s, 4H, CH₂); 2.03 (s, 12H, CH₃).

¹³C{¹H} NMR (toluene-d₈) δ_{C} (ppm): 155.0 (d, C_{Ar} , $^1J_{\text{C-P}} = 42.9$ Hz), 130.1 (d, C_{Ar} , $^2J_{\text{C-P}} = 17.3$ Hz), 128.0 (C_{Ar}), 120.2 (C_{Ar}), 57.9 (CH₂), 45.9 (CH₃).

³¹P NMR (toluene-d₈) δ_{P} (ppm): -20.7.

⁷Li NMR (toluene-d₈) δ_{Li} (ppm): 1.37.

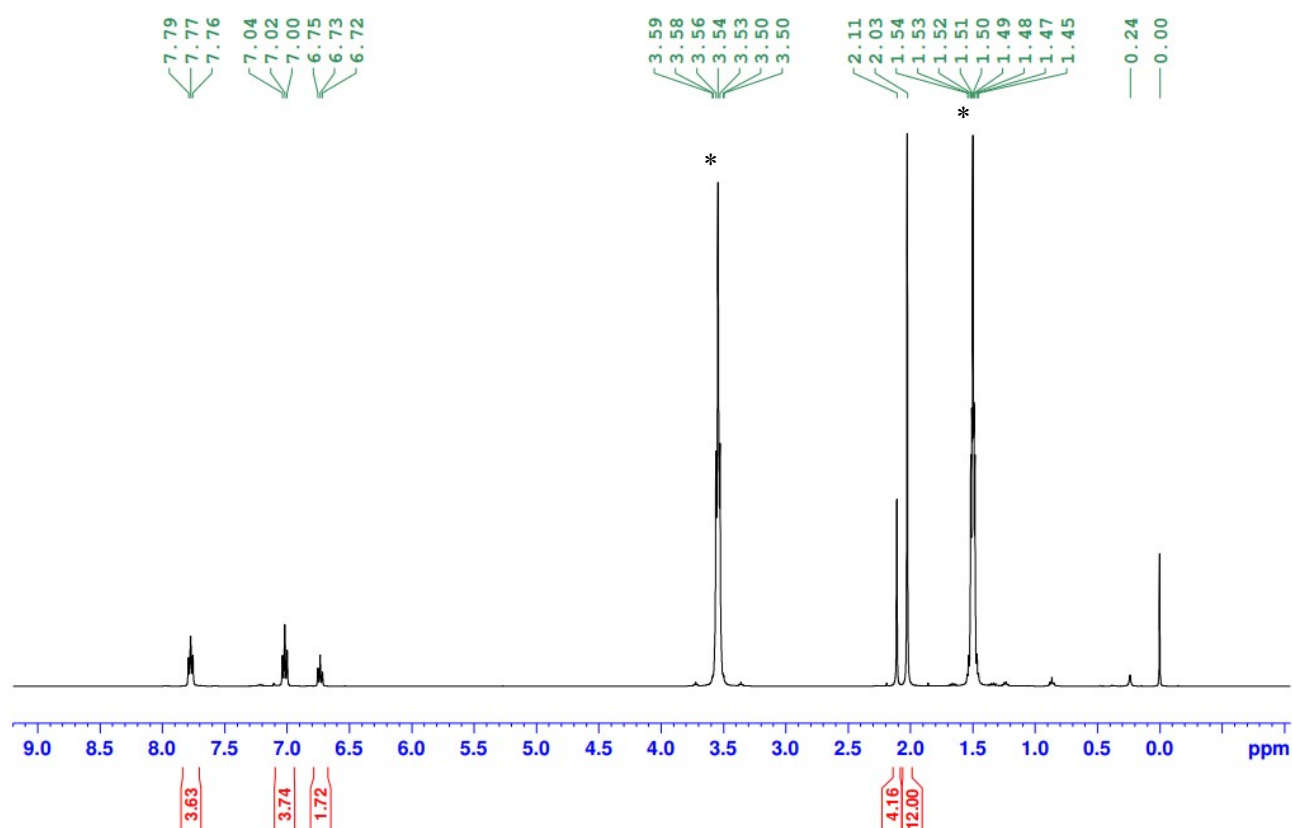


Figure S4 ¹H NMR spectrum of **1** in toluene-d₈. Note THF (*) and TMS (0 ppm).

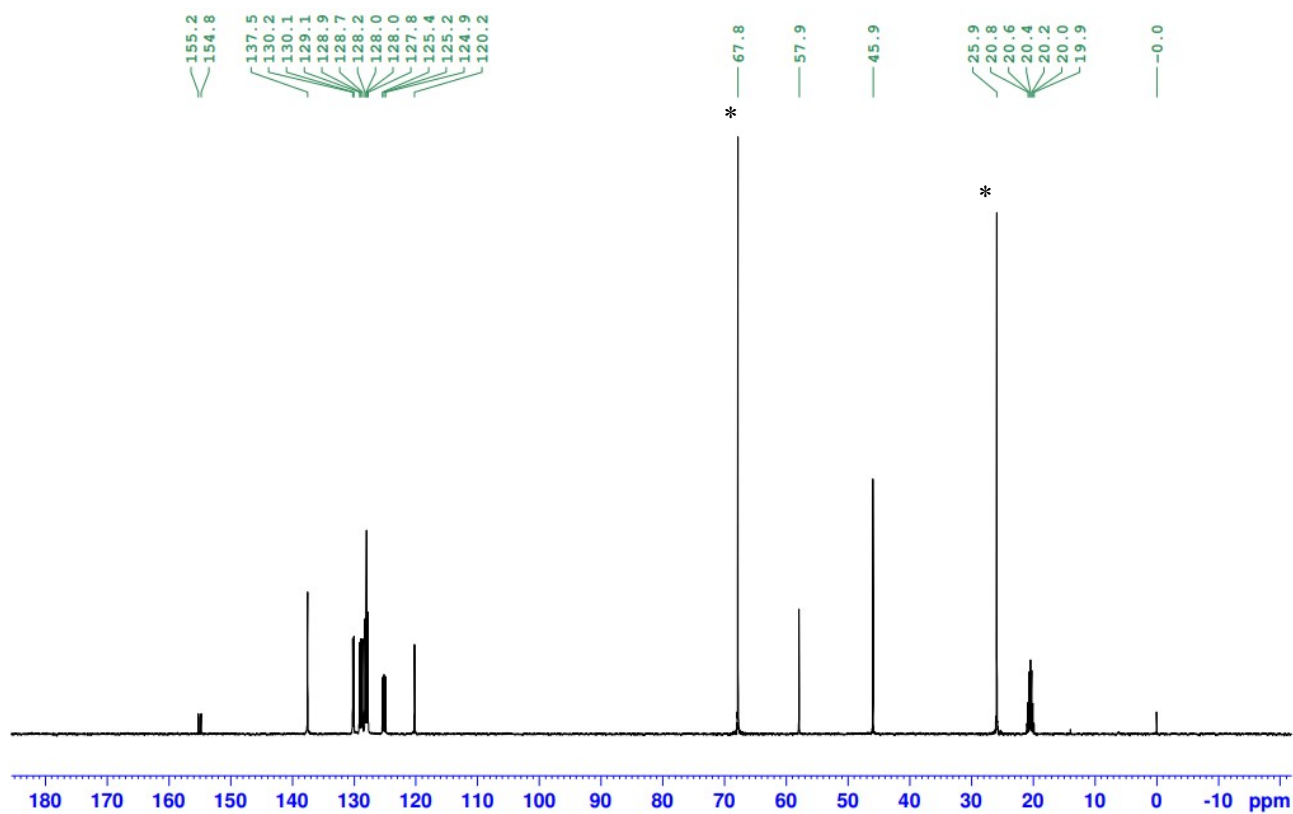


Figure S5 $^{13}\text{C}\{^1\text{H}\}$ NMR spectrum of **1** in toluene- d_8 . Note THF (*) and TMS (0 ppm).

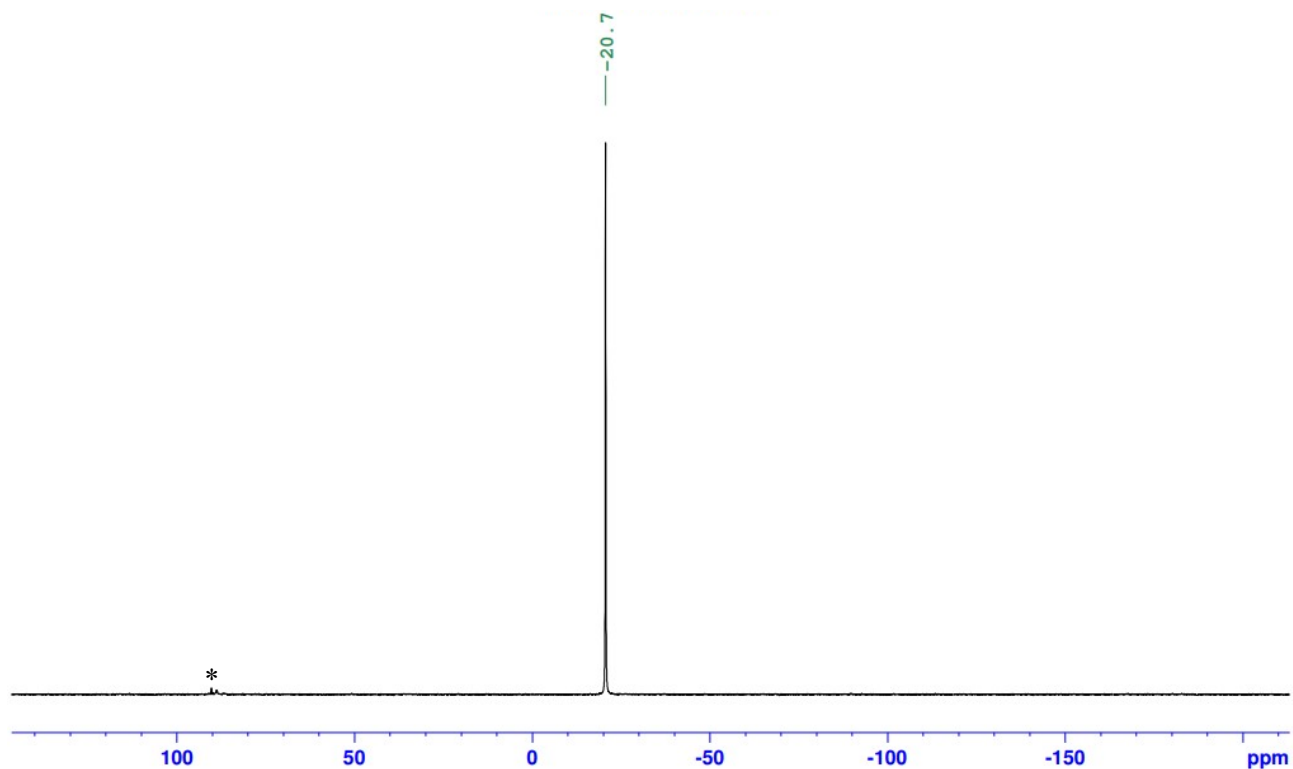


Figure S6 ^{31}P NMR spectrum of **1** in toluene- d_8 . Trace amounts of $\text{Ph}_2\text{P}(\text{OLi})$ and $\text{Ph}_2\text{P}(\text{OK})$ (*) are also present.^{5,6}

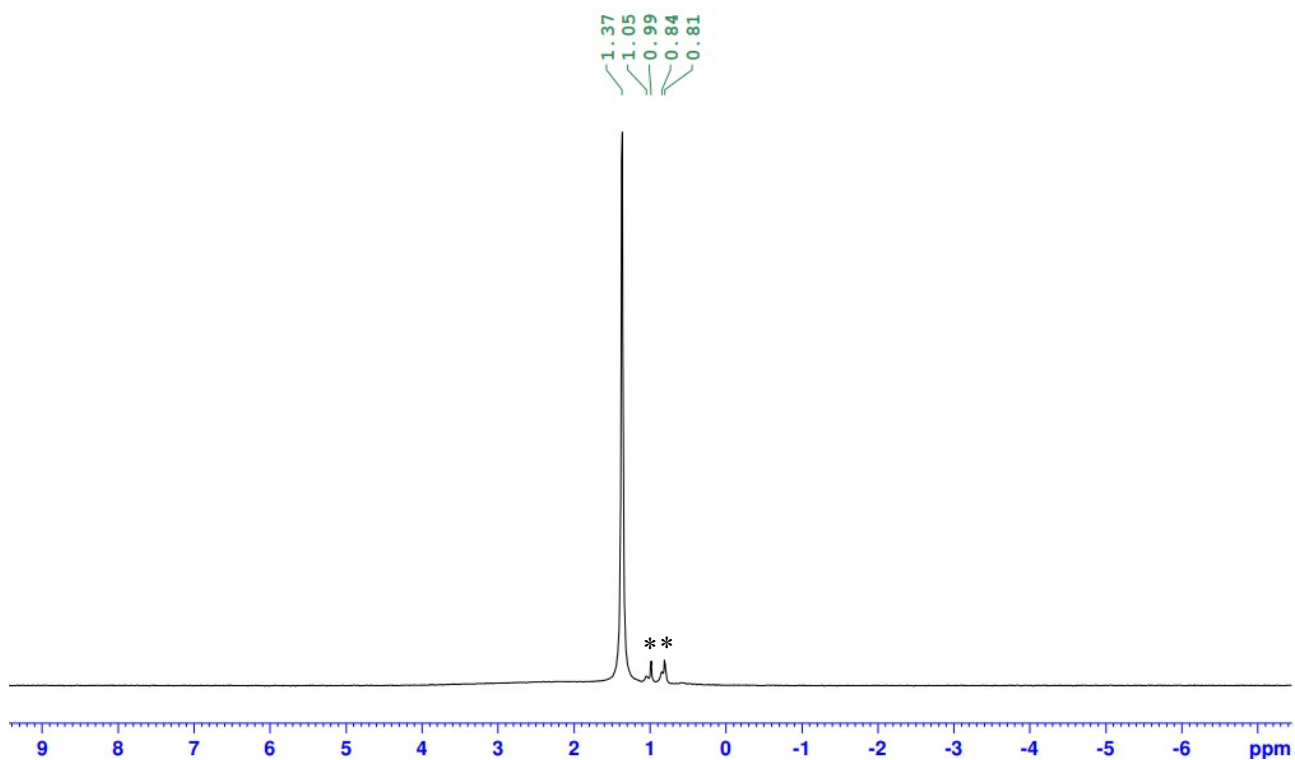


Figure S7 ⁷Li NMR spectrum of **1** in toluene-d₈. Trace amounts of LiPPh₂(THF)₂ and Ph₂P(OLi) (*) are also present.

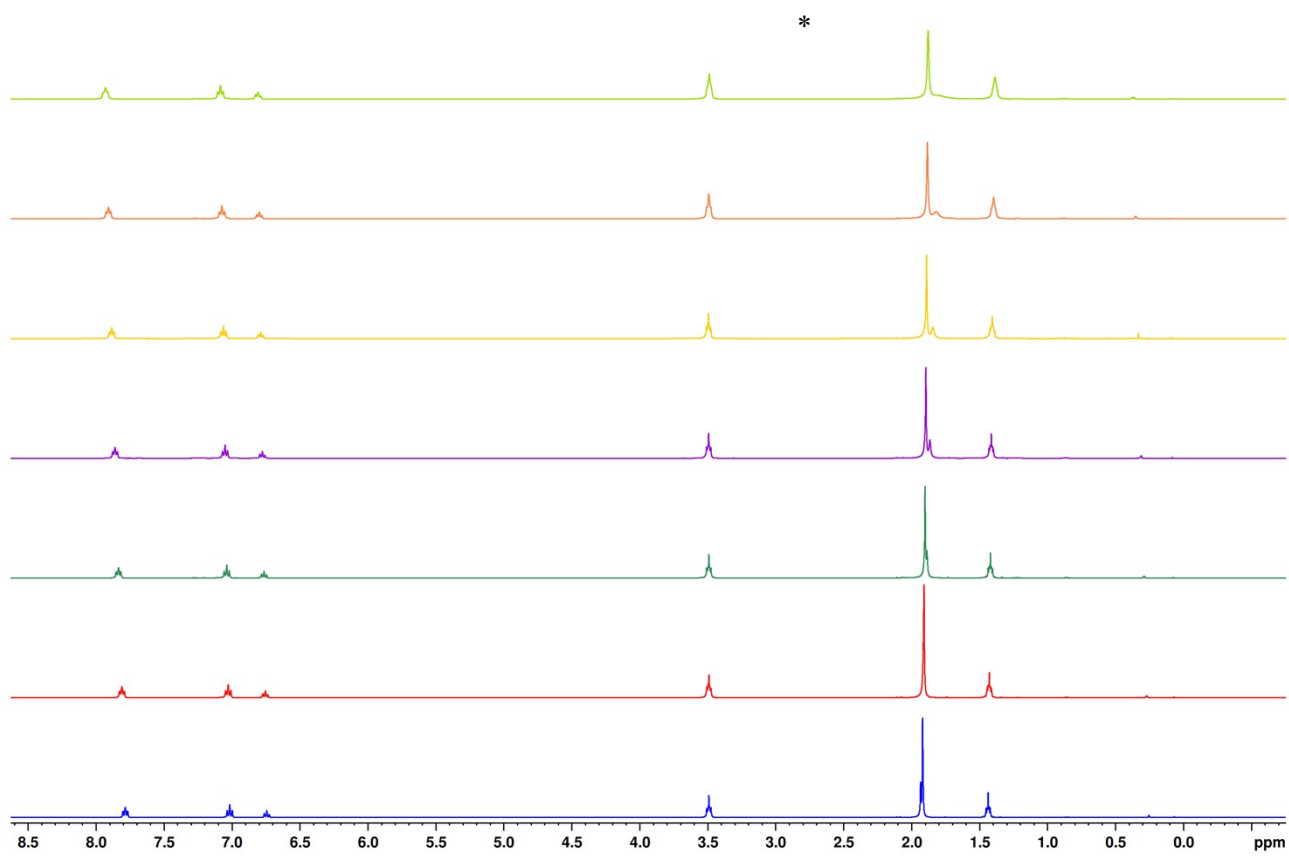


Figure S8 Variable temperature ¹H NMR spectra of **1** in toluene-d₈.

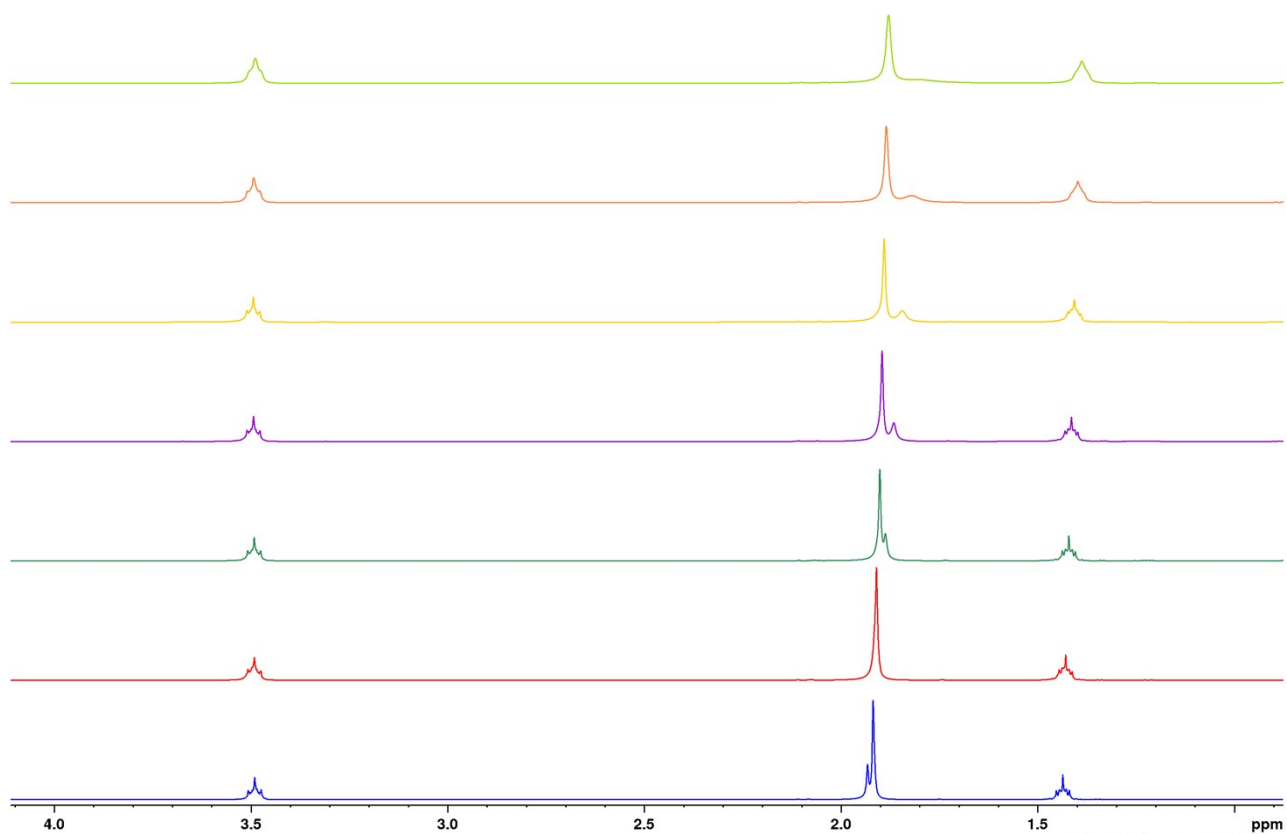


Figure S9 Variable temperature ^1H NMR spectra of **1** in toluene- d_8 , only showing 0-4ppm for the TMEDA coordination.

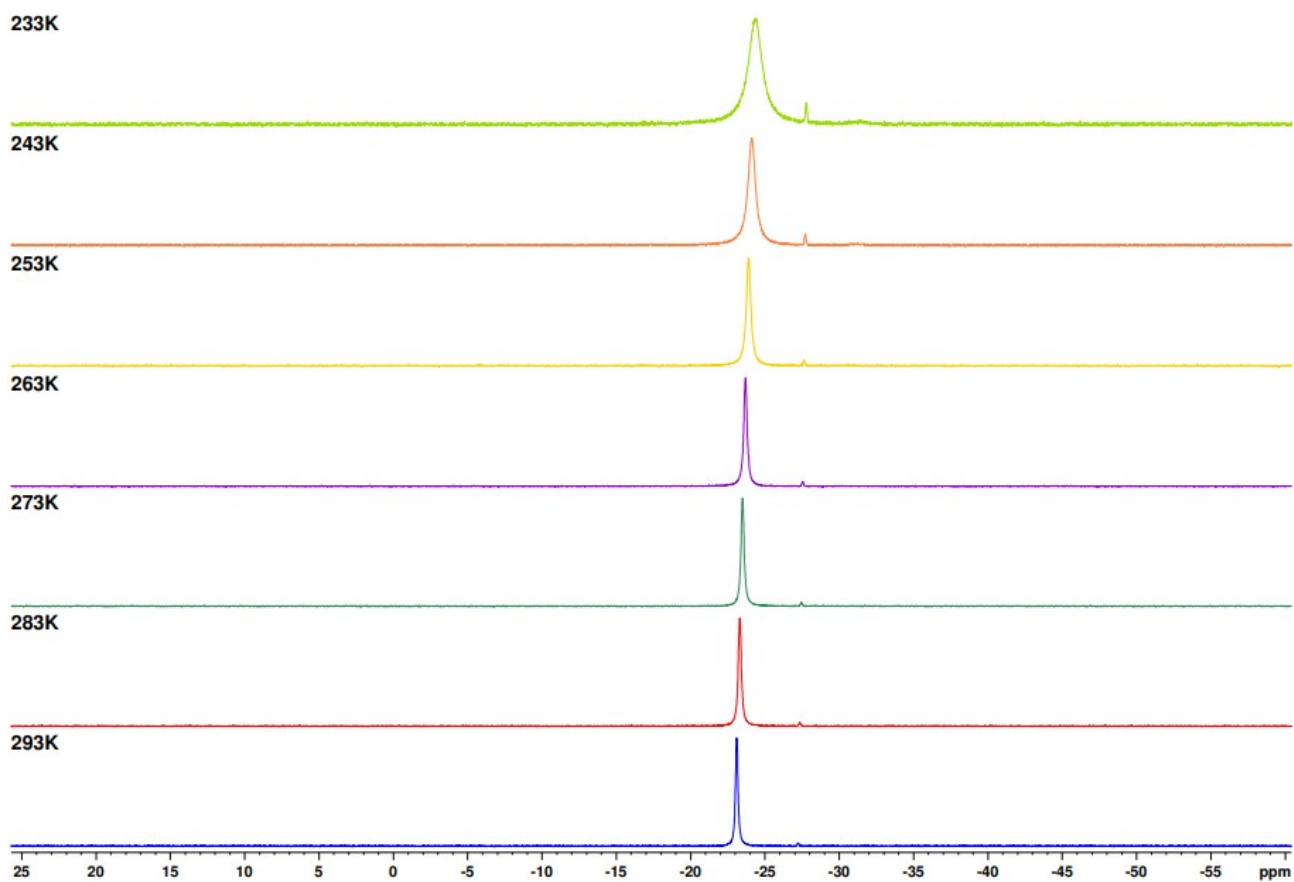


Figure S10 Variable temperature ^{31}P NMR spectra of **1** in toluene- d_8 . Trace amounts of LiPPh_2 (*) are also present.

[(TMEDA)Li(μ -PPh₂)₂K(TMEDA)(THF)] (**1**) – benzene-d₆

¹H NMR (benzene-d₆, 300 K) δ_{H} (ppm): 7.82 (m, 4H, H_{Ar}); 7.05 (m, 4H, H_{Ar}); 6.77 (tt, 2H, H_{Ar} , $^4J_{\text{HH}} = 1.17$ Hz, $^3J_{\text{HH}} = 7.22$ Hz); 2.01 (s, 4H, CH_2); 1.97 (s, 12H, CH_3).

¹³C{¹H} NMR (benzene-d₆) δ_{C} (ppm): 154.9 (d, C_{Ar} , $^1J_{\text{C-P}} = 42.1$ Hz), 130.2 (d, C_{Ar} , $^2J_{\text{C-P}} = 17.16$ Hz), 128.0 (C_{Ar}), 120.3 (C_{Ar}), 57.6 (CH_2), 45.9 (CH_3).

³¹P NMR (benzene-d₆) δ_{P} (ppm): -21.2.

⁷Li NMR (benzene-d₆) δ_{Li} (ppm): 1.48.

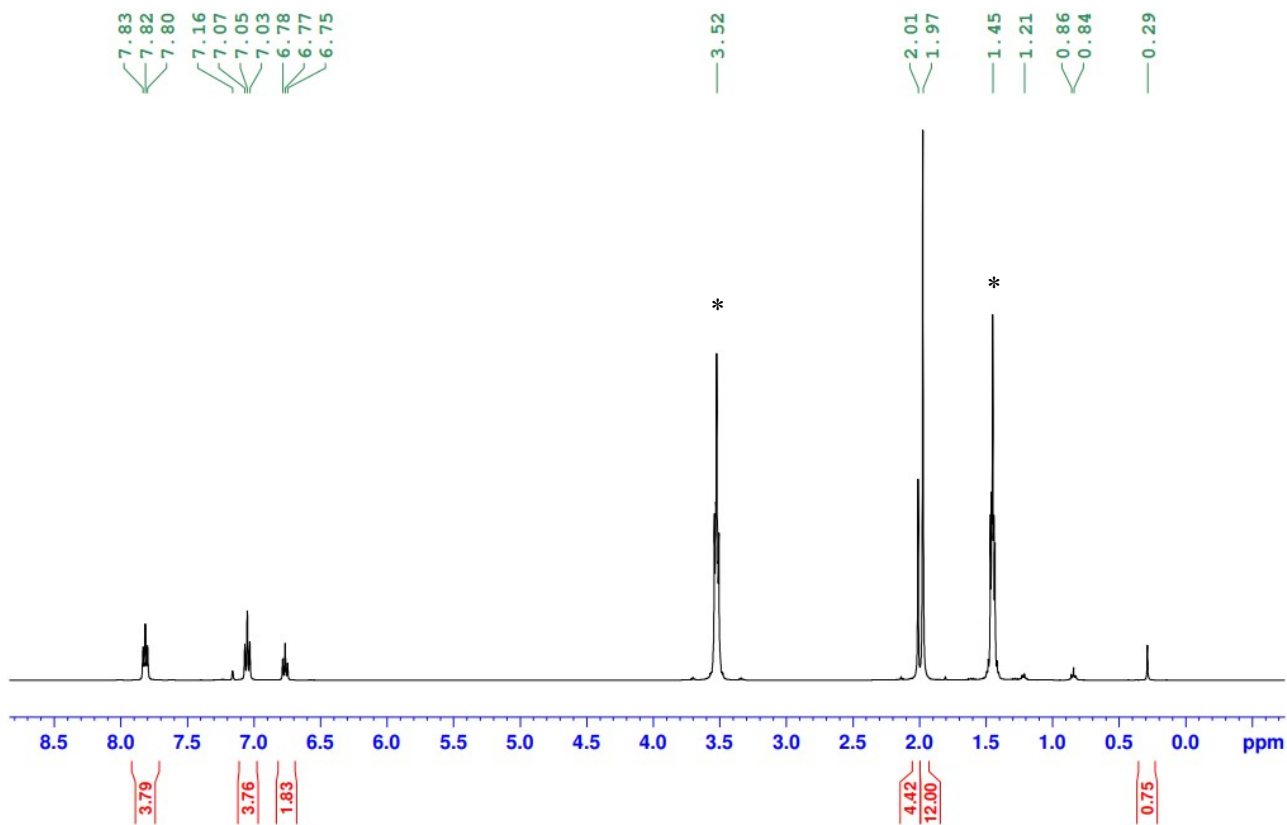


Figure S11 ¹H NMR spectrum of **1** in benzene-d₆. Note THF (*) and small amount of hexane.

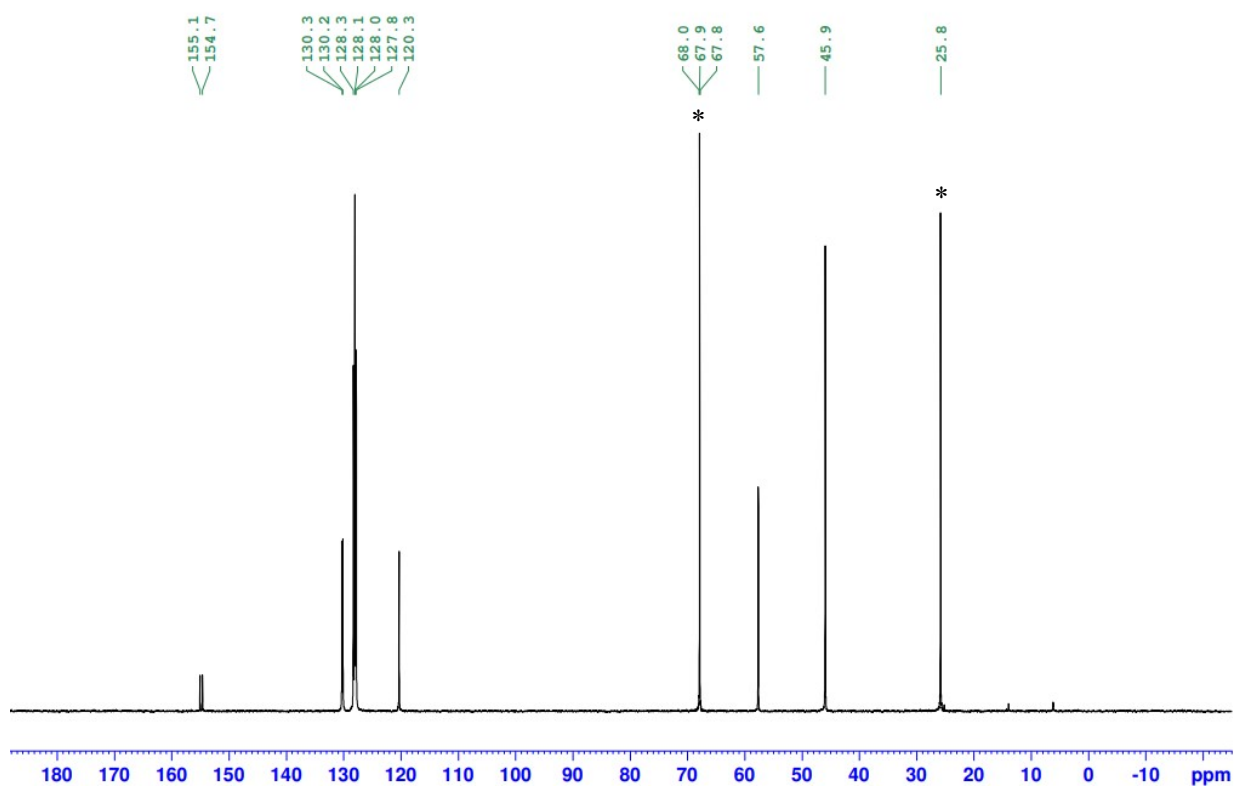


Figure S12 $^{13}\text{C}\{^1\text{H}\}$ NMR spectrum of **1** in benzene- d_6 . Note THF (*) and small amount of hexane.

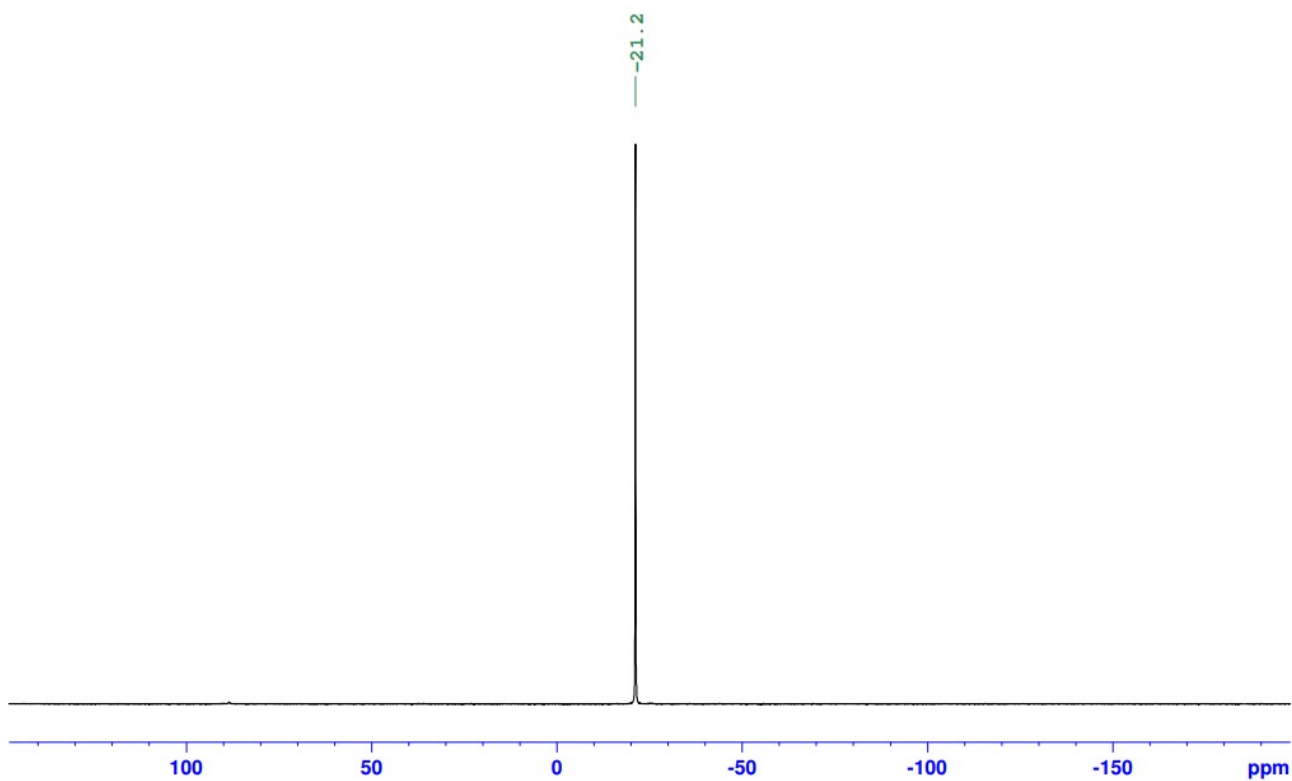


Figure S13 ^{31}P NMR spectrum of **1** in benzene- d_6 .

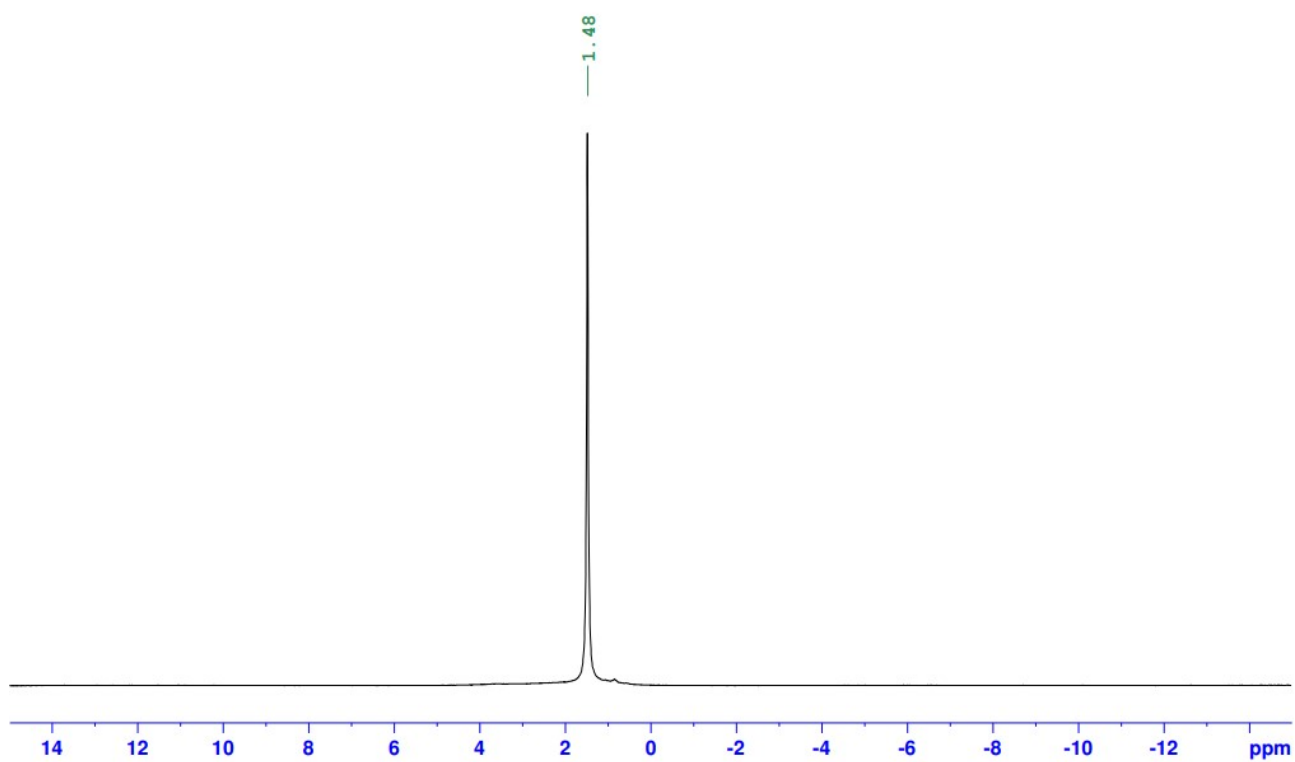


Figure S14 ${}^7\text{Li}$ NMR spectrum of **1** in benzene- d_6 .

^1H DOSY NMR for $[(\text{TMEDA})\text{Li}(\mu\text{-PPh}_2)_2\text{K}(\text{TMEDA})(\text{THF})]$ (**1**) – toluene- d_8

2D ^1H Diffusion-Ordered Spectroscopy (DOSY) spectra were recorded on a Bruker AV400 spectrometer operating at 400.1 MHz for ^1H and measured at 300 K. A 0.1M solution of **1** in 0.5 mL toluene- d_8 and 0.05 mL THF was prepared with the addition of TMS (13.6 μL , 0.1 mmol) as an internal standard. An estimate of the molecular weight (MW) of the species in solution was obtained *via* comparison of the diffusion coefficients of **1** and internal standard TMS to external calibration curves (ECCs) with normalised diffusion coefficients.^{7,8} The ECCs for molecules which diffuse like compact spheres (CS), dissipated spheres and ellipsoids (DSE), extended discs (ED) and a merge of all three were utilised. For species with multiple ^1H signals, the average diffusion coefficient was taken. The accuracy of this estimation is in the range of $\text{MW}_{\text{dif}} \pm 9\%$.^{7,8}

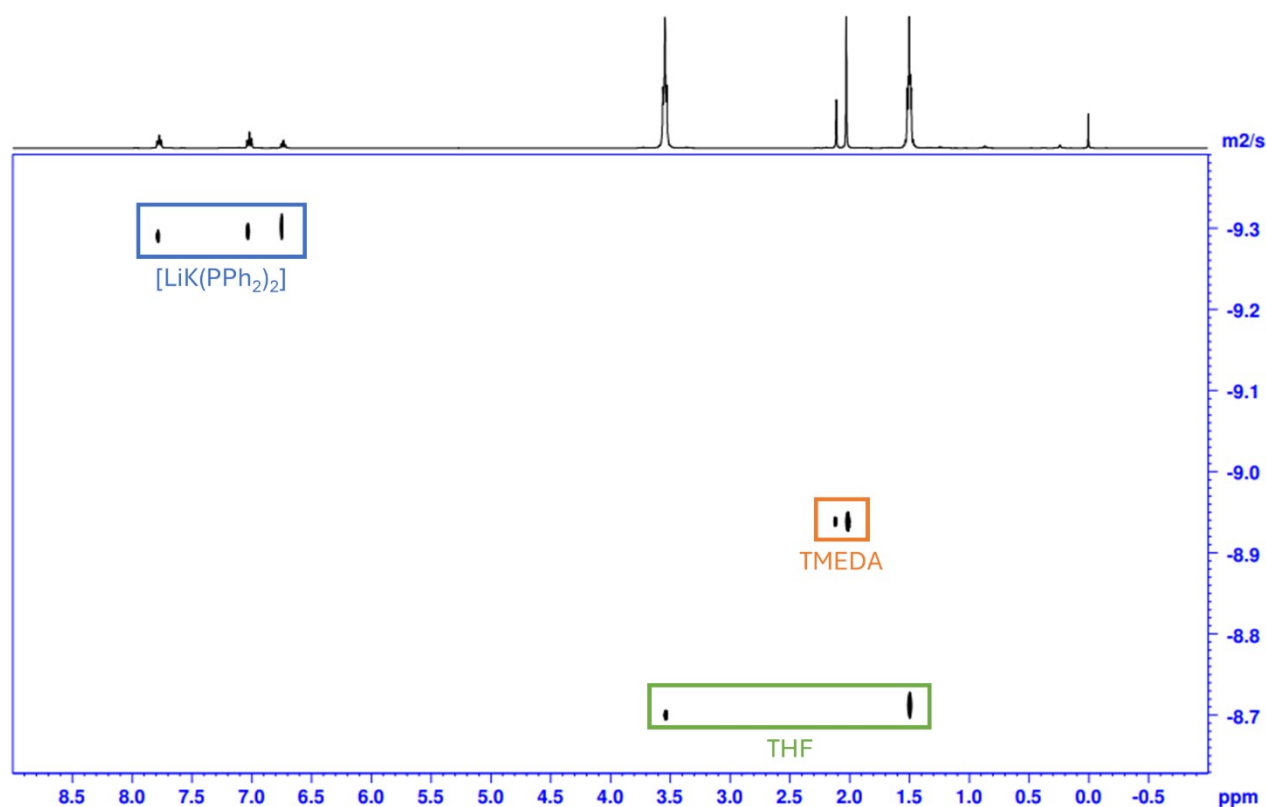


Figure S15 ^1H DOSY NMR of **1** in toluene- d_8 .

Table S1 Diffusion coefficients and corresponding data parameters from 2D ^1H DOSY NMR of **1** in toluene- d_8

Peak Name	F2 (ppm)	lo	error	D ($\text{m}^2 \text{s}^{-1}$)	error	$\log D$
1 LiK	7.781	4.92E+09	7.136E+06	4.98E-10	1.630E-12	-9.30277

2 LiK	7.029	4.68E+09	9.046E+06	4.96E-10	2.164E-12	-9.30452
3 LiK	6.746	2.07E+09	8.638E+06	4.88E-10	4.602E-12	-9.31158
4 THF	3.535	1.41E+09	5.967E+06	1.96E-09	1.798E-12	-8.70774
5 TMEDA	2.115	5.23E+09	6.349E+06	1.13E-09	3.022E-12	-8.94692
6 TMEDA	2.009	2.08E+10	4.091E+07	1.13E-09	4.918E-12	-8.94692
7 THF	1.494	1.40E+10	3.942E+07	1.90E-09	1.163E-11	-8.72125
8 TMS	0.007	8.81E+08	1.024E+07	1.83E-09	4.711E-11	-8.73755
LiK (avg)	–	–	–	4.94E-10	–	-9.30629
TMEDA (avg)	–	–	–	1.13E-09	–	-8.94692
THF (avg)	–	–	–	1.93E-09	–	-8.71450

Table S2 MW and MW_{DOSY} for potential species in **1** and the calculated deviation from their theoretical MW (MW_{diff}).

Species	MW (g mol⁻¹)	ECC	MW_{DOSY} (g mol⁻¹)	MW_{diff} (%)
LiK(PPh ₂) ₂	416	DSE	874	-52
LiK(PPh ₂) ₂ (TMEDA) ₂ (THF)	721	DSE	874	-18
LiK(PPh ₂) ₂ (TMEDA) ₂ (THF)	865	DSE	874	-1
[LiPPh ₂ (TMEDA)] ₂	616	DSE	874	-30
[KPPh ₂ (TMEDA)] ₂	682	DSE	874	-22
TMEDA (avg)	116	DSE	227	-49
THF (avg)	72	CS	82	-12

The data in tables S1 and S2 show the LiK species in solution has a higher experimental MW_{DOSY} (874 g mol⁻¹) than the theoretical value of the LiK(PPh₂)₂(TMEDA)₂(THF) crystal structure (721 g mol⁻¹). This suggests the dynamic exchange of THF and TMEDA. This equilibrium shows it is difficult to accurately state which species are present but the plausible addition of 2 THF ligands in solution gives a MW_{DOSY} very close to the theoretical (865 g mol⁻¹, MW_{diff} = -1%). It can be deduced from figure **S10** that the LiK(PPh₂)₂ core is retained in solution. The calculated MW_{DOSY} for the TMEDA and THF species in solution are higher (227 and 82 g mol⁻¹) than their theoretical values (116 and 72 g mol⁻¹) which further backs up and suggests an equilibrium in solution where THF and TMEDA ligands are fluxional.

[LiPPh₂(TMEDA)]₂ – toluene-d₈ and THF

Synthesised *in situ* on an NMR scale. LiPPh₂ (19.2 mg, 0.1 mmol) was suspended in benzene-d₆ (0.5 mL), then TMEDA (28 μL, 0.2 mmol, 2 eq) was added, forming a yellow solution. THF (0.1 mmol) was added to replicate the solvent mixture used to solubilise **1**.

¹H NMR (benzene-d₆, 300 K) δ_H (ppm): 7.82 (m, 4H, H_{Ar}); 7.09 (m, 4H, H_{Ar}); 6.83 (tt, 2H, H_{Ar}, ⁴J_{HH} = 1.23 Hz, ³J_{HH} = 7.20 Hz); 2.02 (s, 5H, CH₂); 2.00 (s, 15H, CH₃).

³¹P NMR (benzene-d₆) δ_P (ppm): -26.0.

⁷Li NMR (benzene-d₆) δ_{Li} (ppm): 1.16.

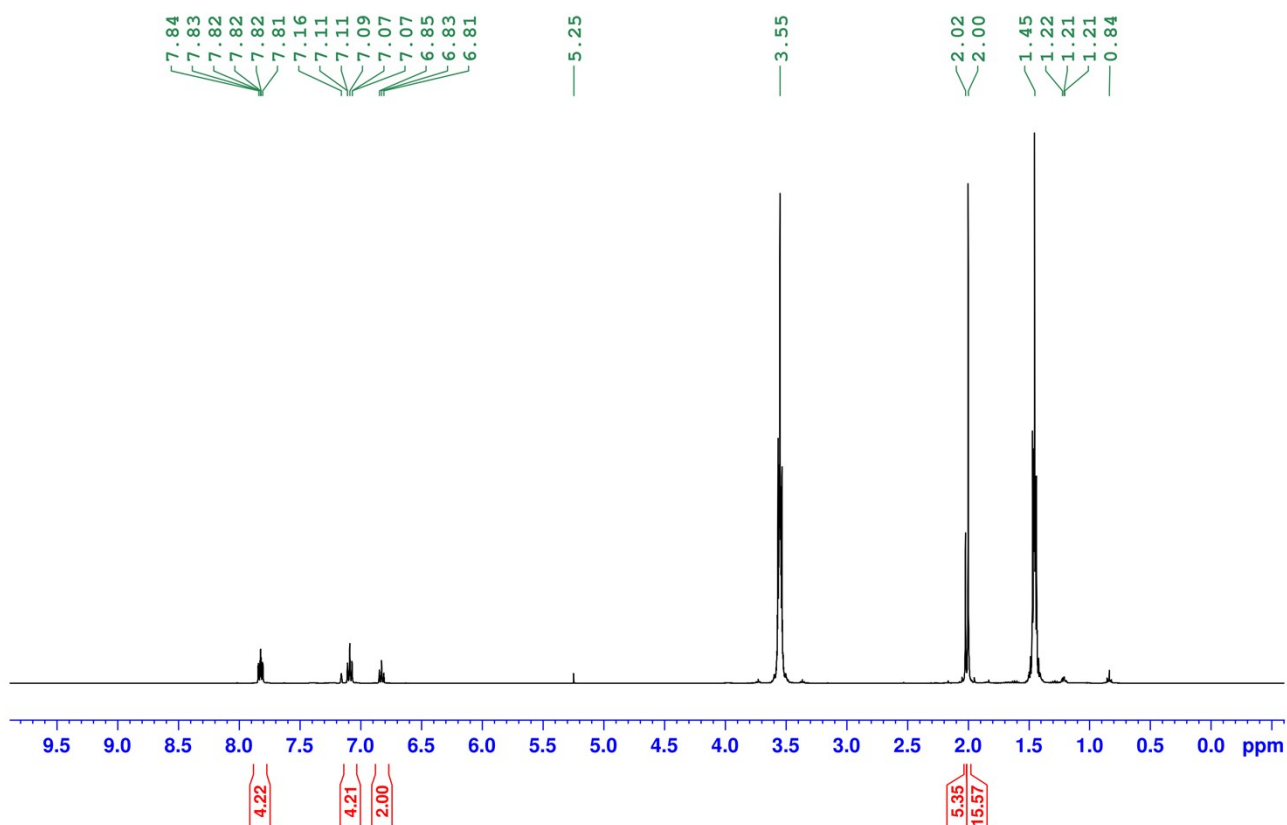


Figure S16 ¹H NMR spectrum of [LiPPh₂(TMEDA)]₂ in benzene-d₆. Note a small amount of hexane and 1,1-diphenylethylene (5.25 ppm).

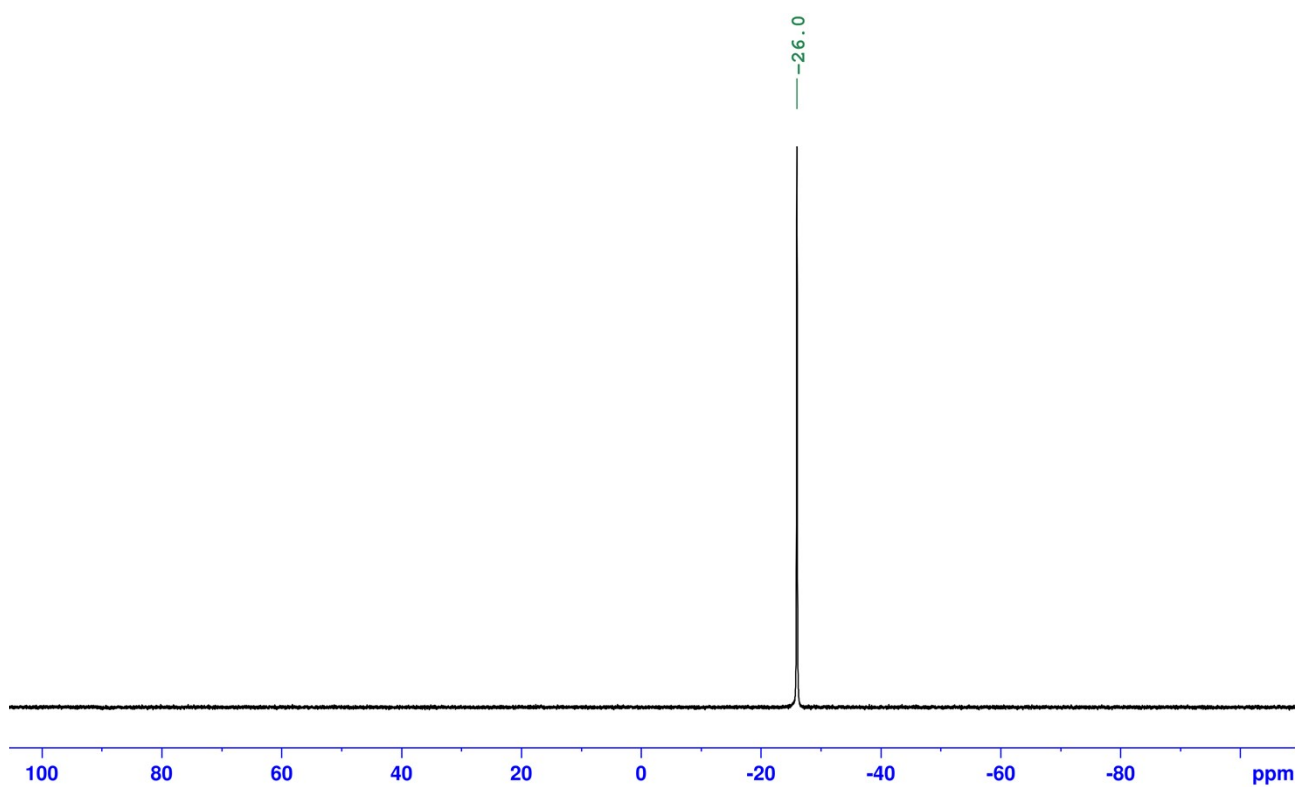


Figure S17 ^{31}P NMR spectrum of $[\text{LiPPh}_2(\text{TMEDA})]_2$ in benzene- d_6 .

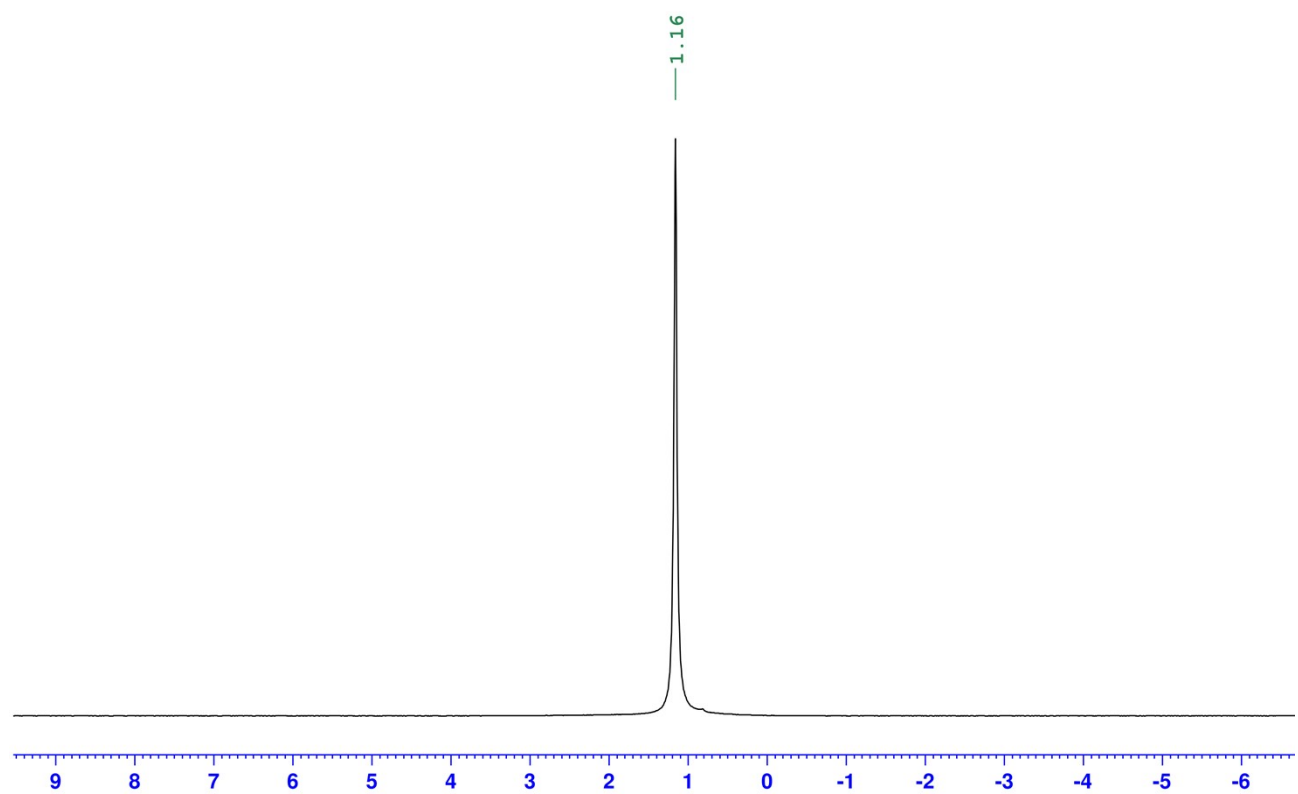


Figure S18 ^7Li NMR spectrum of $[\text{LiPPh}_2(\text{TMEDA})]_2$ in benzene- d_6 .

¹H DOSY NMR for [LiPPh₂(TMEDA)]₂ – toluene-d₈

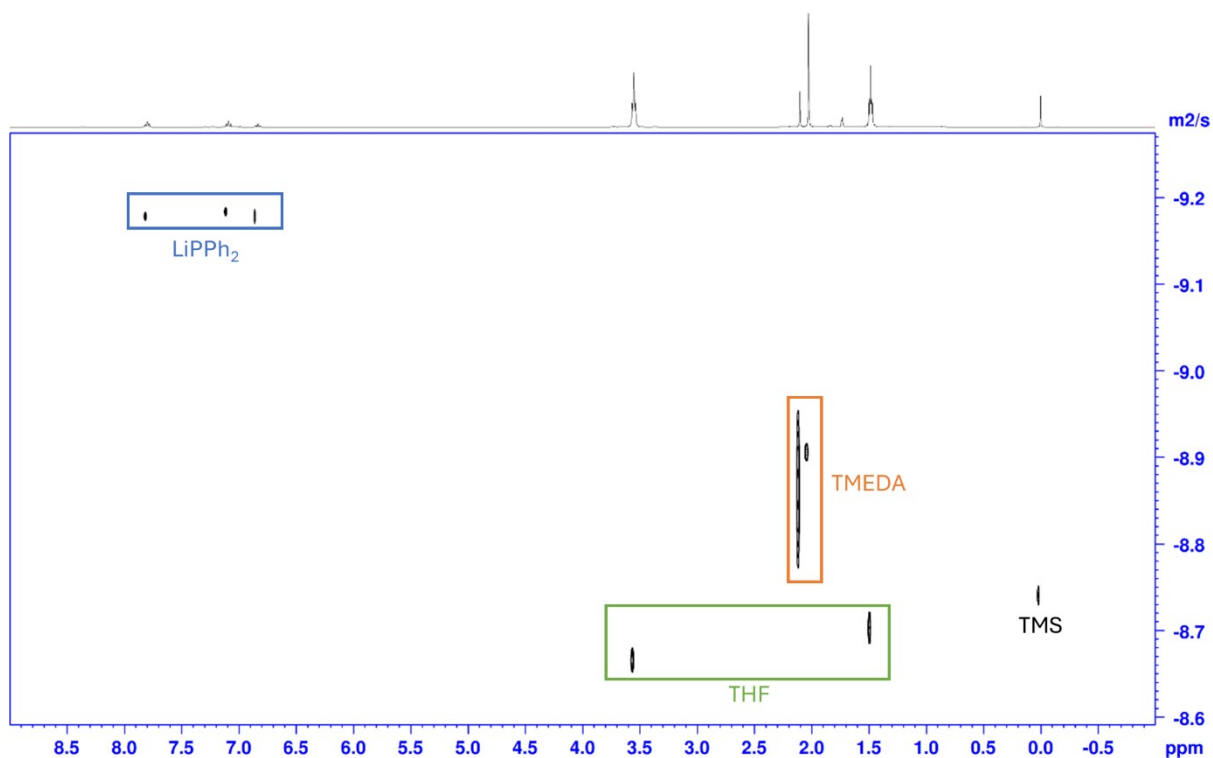


Figure S19 ¹H DOSY NMR spectrum of [LiPPh₂(TMEDA)]₂ in toluene-d₈.

Table S3 Diffusion coefficients and corresponding data parameters from 2D ¹H DOSY NMR of [LiPPh₂(TMEDA)]₂ in toluene-d₈

Peak Name	F2 (ppm)	<i>D</i> (m ² s ⁻¹)	error	log <i>D</i>
1 LiPPh₂	7.816	6.47E-10	5.751E-12	-9.18910
2 LiPPh₂	7.116	6.38E-10	6.369E-12	-9.19518
3 LiPPh₂	6.859	6.47E-10	2.084E-11	-9.18910
4 THF	3.563	2.14E-09	4.285E-11	-8.66959
5 TMEDA	2.116	1.35E-09	1.800E-10	-8.86967
6 TMEDA	2.043	1.22E-09	1.302E-11	-8.91364
7 THF	1.492	1.94E-09	5.259E-11	-8.71220
8 TMS	0.019	1.78E-09	5.720E-11	-8.74957
LiK (avg)	–	4.94E-10	–	-9.19111
TMEDA (avg)	–	1.13E-09	–	-8.89110
THF (avg)	–	1.93E-09	–	-8.69036

Species	MW (g mol ⁻¹)	ECC	MW _{DOSY} (g mol ⁻¹)	MW _{dif}
[LiPPh ₂ (TMEDA)] ₂	616	CS	693	-11
[LiPPh ₂ (TMEDA)] ₂	616	Merge	571	8
[LiPPh ₂ (TMEDA)] ₂	616	DSE	542	14
TMEDA (avg)	116	DSE	176	-34
THF (avg)	72	CS	70	3

[KPh₂(TMEDA)]_n – toluene-d₈ and THF

Synthesised *in situ* on an NMR scale. KPh₂ (22.4 mg, 0.1 mmol) was suspended in benzene-d₆ (0.5 mL), then TMEDA (28 μL, 0.2 mmol, 2 eq) was added, forming a amber solution. THF (0.1 mmol) was added to replicate the solvent mixture used to solubilise **1**.

¹H NMR (benzene-d₆, 300 K) δ_H (ppm): 7.79 (m, 4H, H_{Ar}); 7.00 (t, 4H, H_{Ar}, ³J_{HH} = 7.46 Hz); 6.71 (m, 2H, H_{Ar}); 2.20 (s, 5H, CH₂); 2.03 (s, 15H, CH₃).

³¹P NMR (benzene-d₆) δ_p (ppm): -15.7.

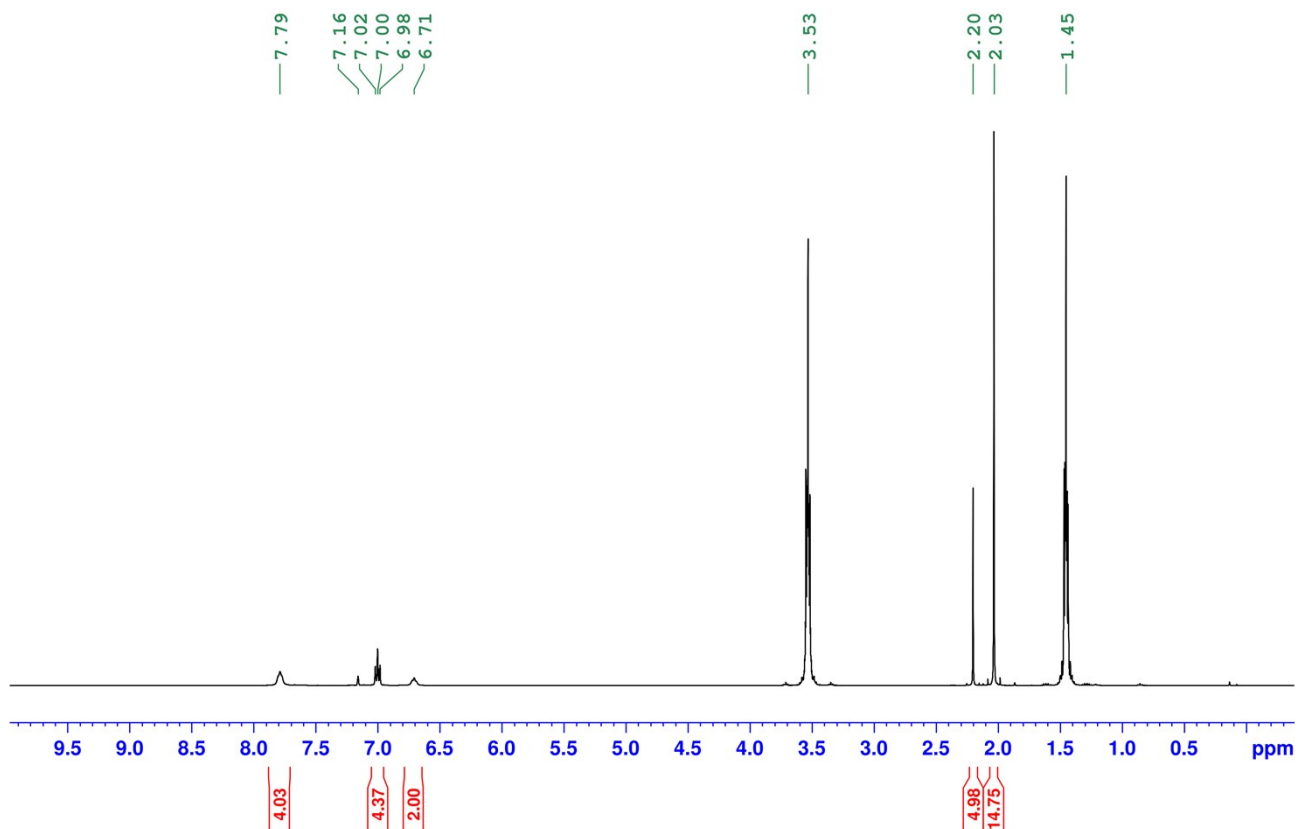


Figure S20 ¹H NMR spectrum of [KPh₂(TMEDA)]_n in benzene-d₆. Note small amounts of hexane and HMDS(H) (0.1 ppm).

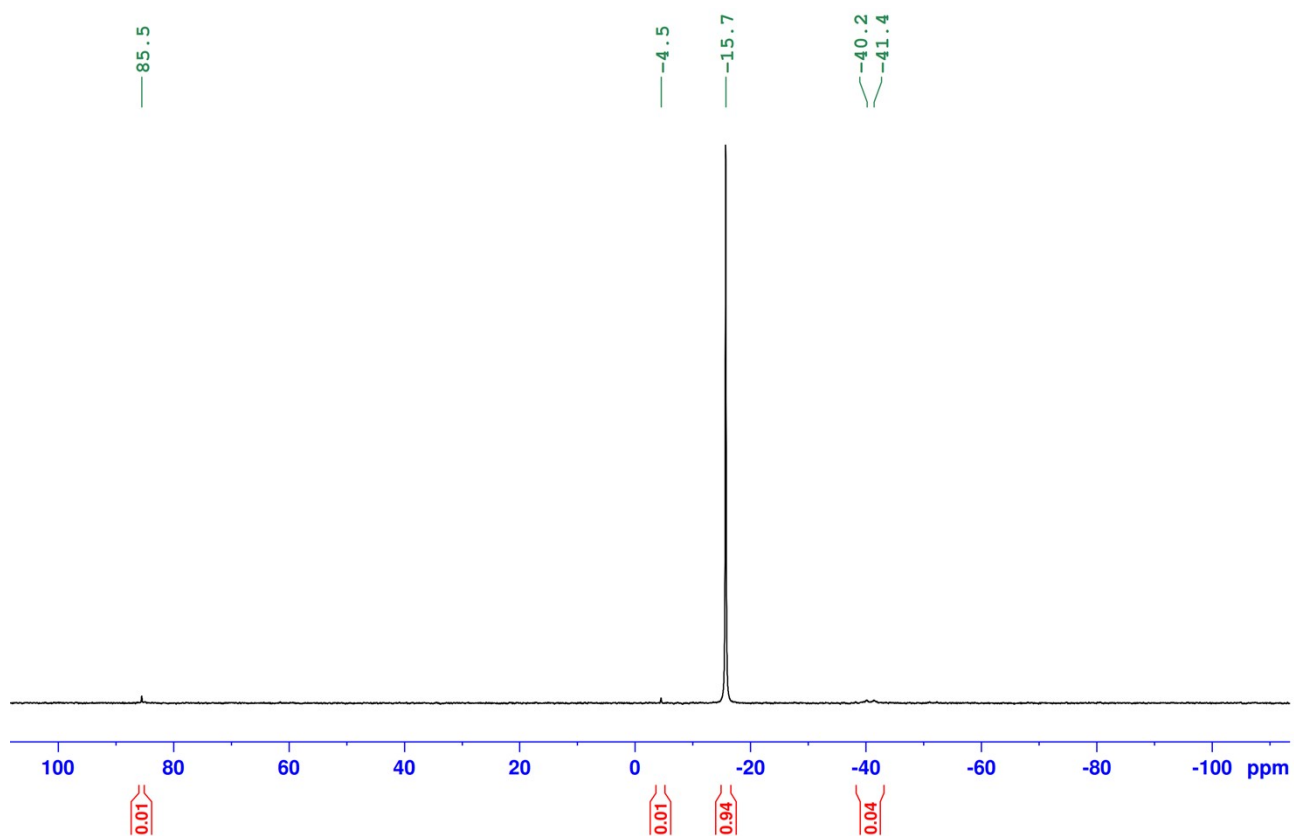


Figure S21 ^1H NMR spectrum of $[\text{KPh}_2(\text{TMEDA})]_n$ in benzene- d_6 . Note small amounts byproducts including $\text{Ph}_2\text{P}(\text{OK})$ (85.5 ppm), HPPh_2 (-40.8 ppm) and an unidentified product (-4.6 ppm).

^1H DOSY NMR for $[\text{KPh}_2(\text{TMEDA})]_n$ – toluene- d_8

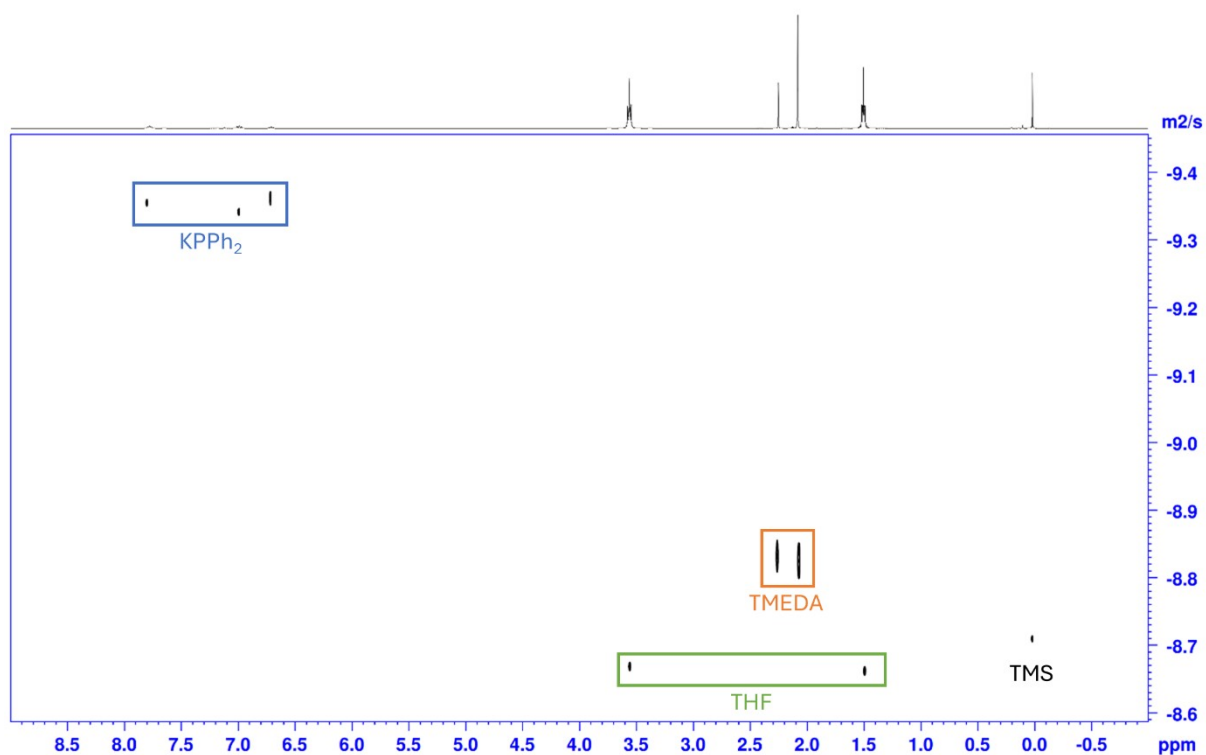


Figure S22 ^1H DOSY NMR spectrum of $[\text{KPh}_2(\text{TMEDA})]_n$ in toluene- d_8 .

Table S4 Diffusion coefficients and corresponding data parameters from 2D ^1H DOSY NMR of $[\text{KPPh}_2(\text{TMEDA})]_n$ in toluene- d_8

Peak Name	F2 (ppm)	lo	error	D ($\text{m}^2 \text{s}^{-1}$)	error	log D
1 KPPh₂	7.776	2.08E+08	4.176E+05	4.32E-10	1.949E-12	-9.36452
2 KPPh₂	6.994	2.08E+08	2.993E+05	4.38E-10	1.411E-12	-9.35852
3 KPPh₂	6.708	9.46E+07	7.137E+05	4.27E-10	7.234E-12	-9.36957
4 THF	3.554	5.13E+08	6.770E+05	2.12E-09	5.993E-12	-8.67366
5 TMEDA	2.261	4.59E+08	7.252E+06	1.44E-09	4.926E-11	-8.84164
6 TMEDA	2.087	1.43E+09	1.849E+07	1.45E-09	4.056E-11	-8.83863
7 THF	1.504	5.23E+08	1.687E+06	2.15E-09	1.478E-11	-8.66756
8 TMS	0.020	1.48E+08	4.619E+05	1.94E-09	1.299E-11	-8.71220
KPPh₂ (avg)	–	–	–	4.32E-10	–	-9.36421
TMEDA	–	–	–	1.45E-09	–	-8.84013
THF (avg)	–	–	–	2.14E-09	–	-8.67060

Species	MW (g mol^{-1})	ECC	MW _{DOSY} (g mol^{-1})	MW _{dif}
$[\text{KPPh}_2(\text{TMEDA})]_2$	682	DSE	1195	-43
$[\text{KPPh}_2(\text{TMEDA})]_3$	1023	DSE	1195	-14
$[\text{KPPh}_2(\text{TMEDA})]_4$	1364	DSE	1195	14
TMEDA (avg)	116	DSE	167	-31
THF (avg)	72	CS	76	-5

2. Single Crystal X-Ray Crystallography (SC-XRD)

2.1 General Crystallographic Information

Crystallographic data were measured with a Rigaku Synergy-I diffractometer using monochromated ($\lambda = 1.54184 \text{ \AA}$) Cu-K α radiation. Crystals were layered with perfluoropolyalkylether oil prior to mounting on the X-ray diffractometer. All data was collected at 100K and processed with CrysAlisPro⁹ software. Structures were solved using the ShelXT¹⁰ program and refined to convergence against F^2 and all reflections with ShelXL-2018¹¹; both with the software Olex2.¹²

Parts of the structure of compound **1** was treated as disordered over two sites one THF ligand and one TMEDA [(CH₃)₂NCH₂CH₂N(CH₃)₂] ligand were disordered. Appropriate restraints and constraints were applied to these disordered groups to ensure that they approximated to normal geometric and displacement behaviours. Selected crystallographic data and refinement parameters are presented in table S3 and full details are available in cif format from the CCDC as deposition number 2434958.

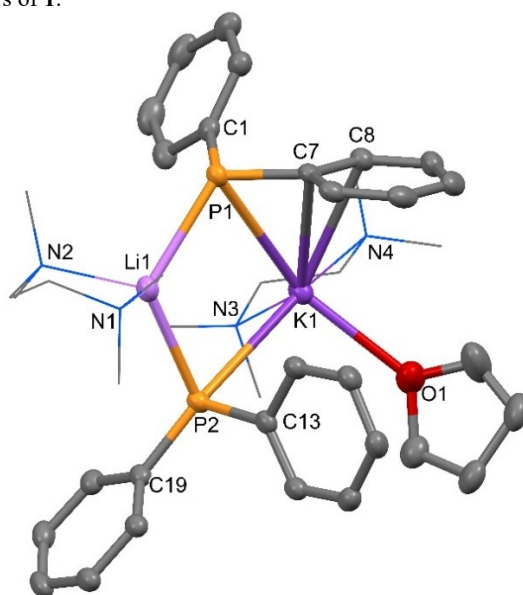
Table S5. Selected Crystallographic and Refinement Parameters.

Compound	1
CCDC Identifier	2434958
Empirical formula	KLiP ₂ ON ₄ C ₄₀ H ₆₀
Formula weight	720.90
Temperature/K	100(2)
Crystal system	triclinic
Space group	P-1
a/Å	12.0377(1)
b/Å	12.2718(1)
c/Å	14.9623(1)
$\alpha/^\circ$	90.125(1)
$\beta/^\circ$	107.078(1)
$\gamma/^\circ$	100.987(1)
Volume/Å ³	2070.12(3)
Z	2
$\rho_{\text{calc}}/\text{cm}^3$	1.157
μ/mm^{-1}	2.106
F(000)	776
2 θ range for data collection/ $^\circ$	6.192 to 145.88
Reflections collected	41792
Independent reflections	8218
<i>Rint</i>	0.0394
Data/restraints/parameters	8218/218/534
Goodness-of-fit on F^2	1.051
Final R indexes [$I \geq 2\sigma(I)$]	$R_1 = 0.0391$, $wR_2 = 0.1085$
Final R indexes [all data]	$R_1 = 0.0400$, $wR_2 = 0.1093$
Largest diff. peak/hole / e Å ⁻³	0.621/-0.424

2.2 Selected Bond Lengths and Angles

1 – [LiK(PPh₂)₂(TMEDA)₂(THF)]

Table S6 Selected Bond Parameters of **1**.



Selected Bond Lengths (Å)		Selected Bond Angles (°)			
Li1–P1	2.602(2)	P2–Li1–P1	116.36(9)	N3–K1–N4	64.26(10)
Li1–P2	2.599(3)	N1–Li1–P1	115.80(11)	N3–K1–C7	144.08(6)
Li1–N1	2.130(3)	N1–Li1–P2	108.68(10)	N3–K1–C8	138.40(6)
Li1–N2	2.126(3)	N2–Li1–P1	106.57(10)	N4–K1–P1	117.00(11)
K1–P1	3.4466(5)	N2–Li1–P2	117.94(11)	N4–K1–P2	151.04(10)
K1–P2	3.2419(4)	N2–Li1–N1	88.58(10)	N4–K1–C7	108.35(10)
K1–N3	2.839(2)	P2–K1–P1	82.649(11)	N4–K1–C8	84.98(10)
K1–N4	2.906(10)	P2–K1–C7	99.18(3)	C7–K1–P1	31.15(3)
K1–O1	2.6892(14)	O1–K1–P1	138.36(4)	C8–K1–P1	51.49(3)
K1–C7	3.2983(14)	O1–K1–P2	93.48(3)	C8–K1–P2	123.51(3)
K1–C8	3.1566(14)	O1–K1–N3	103.60(7)	C8–K1–C7	25.06(4)
P1–C1	1.8286(15)	O1–K1–N4	85.13(10)	K1–P1–Li1	77.99(6)
P1–C7	1.8168(14)	O1–K1–C7	110.90(4)	C7–P1–C1	103.20(6)
P2–C13	1.8244(15)	O1–K1–C8	100.73(4)	K1–P2–Li1	81.99(6)
P2–C19	1.8127(14)	N3–K1–P1	117.62(6)	C19–P2–C13	105.05(7)
C7–C8	1.407(2)	N3–K1–P2	88.18(4)	C8–C7–P1	126.11(11)

Li–P and K–P distances exceed the sum of their covalent radii [Li–P = 2.44 Å; K–P = 3.07 Å]¹³ but are within vdW radii [Li–P = 3.61 Å; K–P = 4.55 Å].¹⁴

2.3 Low Hapticity Analysis

For a six-carbon aryl ring there is an idealised position for where a metal coordinating to it sits, depending on hapticity η^1 through to η^6 .

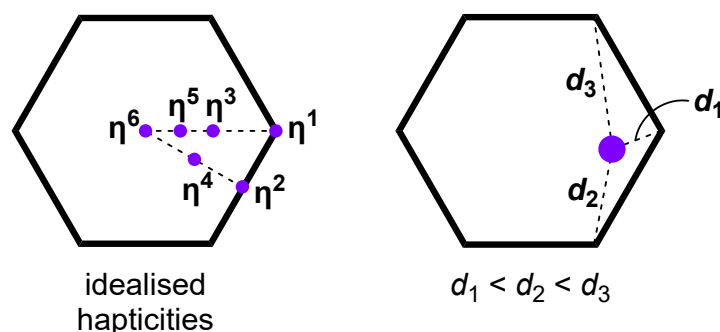
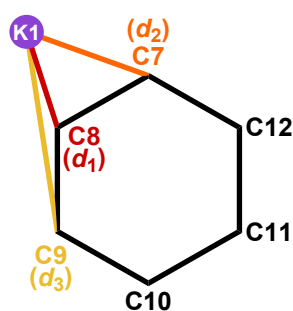


Figure S23 Plan projection of the idealised positions according to η^n hapticities for $n = 1 - 6$; and the definitions of d_1 , d_2 and d_3 according to the position of the metal.

It can be difficult to quantify and classify lower hapticity ($\eta^1 - \eta^3$) aryl interactions, however a systematic method has been developed by Alvarez and co-workers.¹⁵ This is done by taking the three shortest M–C distances (d_1 , d_2 and d_3 , where $d_1 < d_2 < d_3$) and deriving two ratios from these values: ρ_1 and ρ_2 . The relation of ρ_1 and ρ_2 dictates the hapticity of the π coordination such that η^1 hapticity is consistent with $\rho_1 \approx \rho_2 \gg 1$, η^2 when $d_1 \approx d_2 < d_3$ and $\rho_1 > \rho_2 \approx 1$, and η^3 when $d_1 \approx d_2 \approx d_3$ and $\rho_1 \approx \rho_2 \approx 1$. Applying their criteria for a geometric analysis of **1** and to reinforce the crystallographic evidence of a η^2 interaction, the calculated ρ_1 (1.04) and ρ_2 (1.25) values predicts that K1 exhibits η^2 coordination to the π system.

Table S7 K1–C bond lengths and the calculated ρ_1 and ρ_2 for **1**.



K1–C dist.	Å
K1–C7	3.298 (d_2)
K1–C8	3.157 (d_1)
K1–C9	3.947 (d_3)
K1–C10	4.704
K1–C11	4.808
K1–C12	4.200

$$\rho_1 = \frac{3.298}{3.157} = \mathbf{1.044}$$

$$\rho_2 = \frac{3.947}{3.157} = \mathbf{1.250}$$

3. Catalytic Hydrophosphination

3.1 Hydrophosphination of 1,1-DPE Using **1**

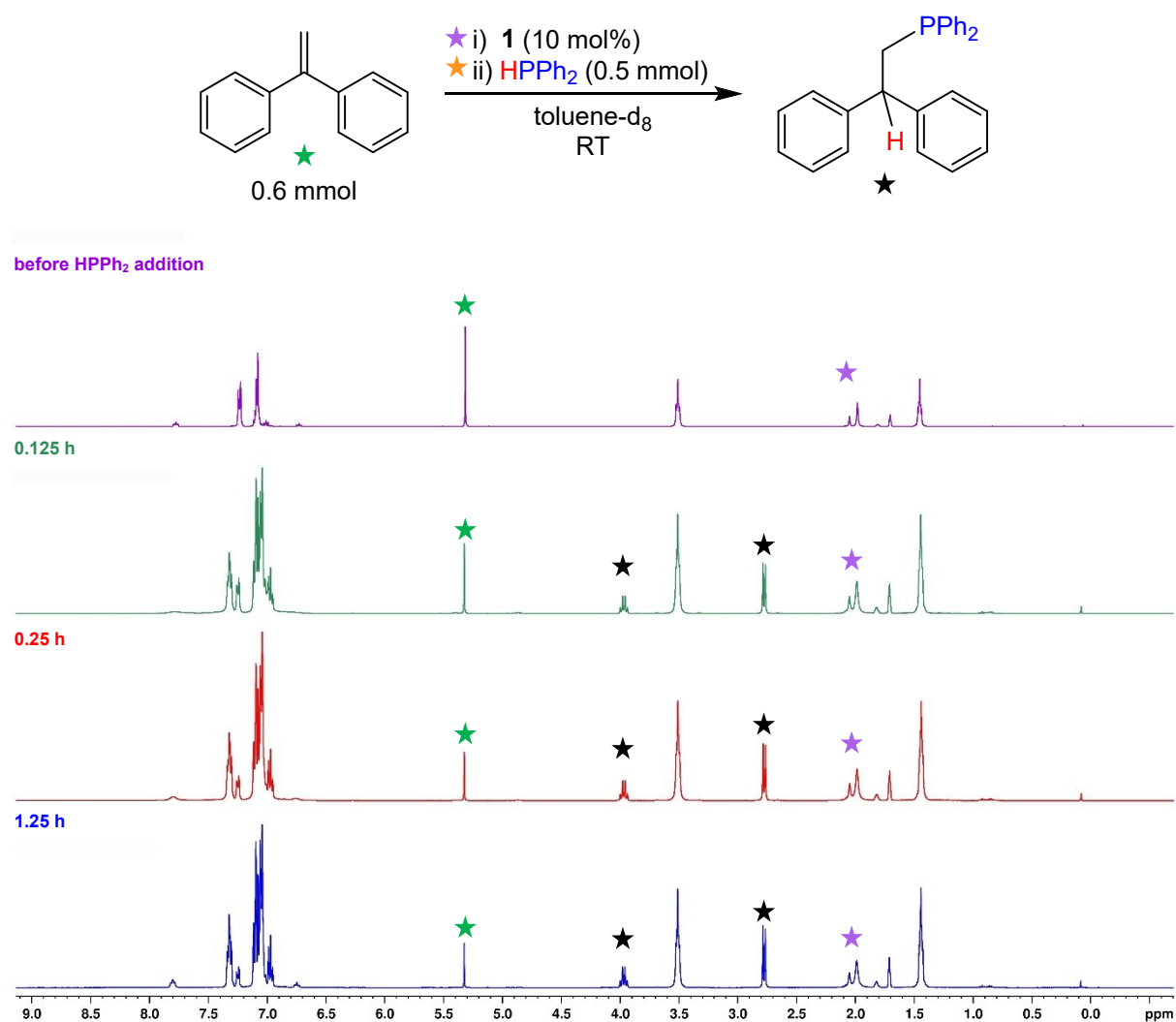


Figure S24 Stacked ¹H NMR spectra of the catalytic hydrophosphination reaction of 1,1-diphenylethylene by **1** over time. Adamantane (0.035 mmol) was added as internal standard to calculate conversion. For solubility, 0.06 mL THF was added. Purple star = catalyst, green star = 1,1-diphenylethylene, black star = product.

before HPPh₂ addition

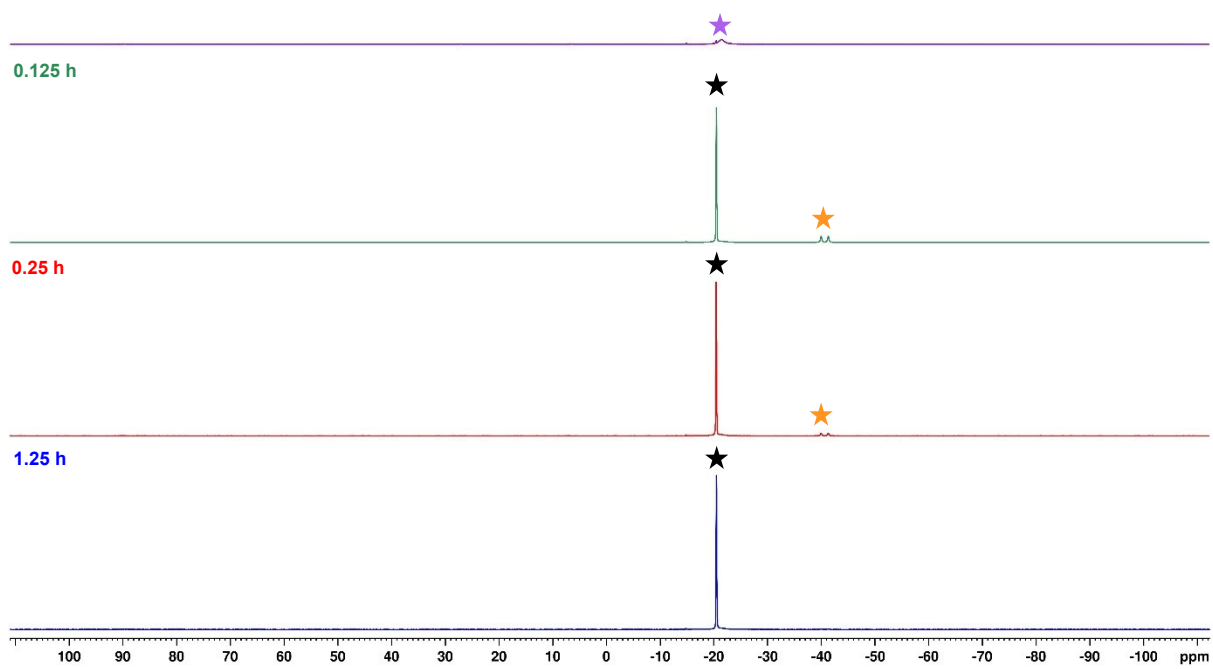


Figure S25 Stacked ³¹P NMR spectra of the catalytic hydrophosphination reaction of 1,1-diphenylethylene by **1** over time. Purple star = catalyst, orange star = HPPh₂, black star = product.

before HPPH₂ addition

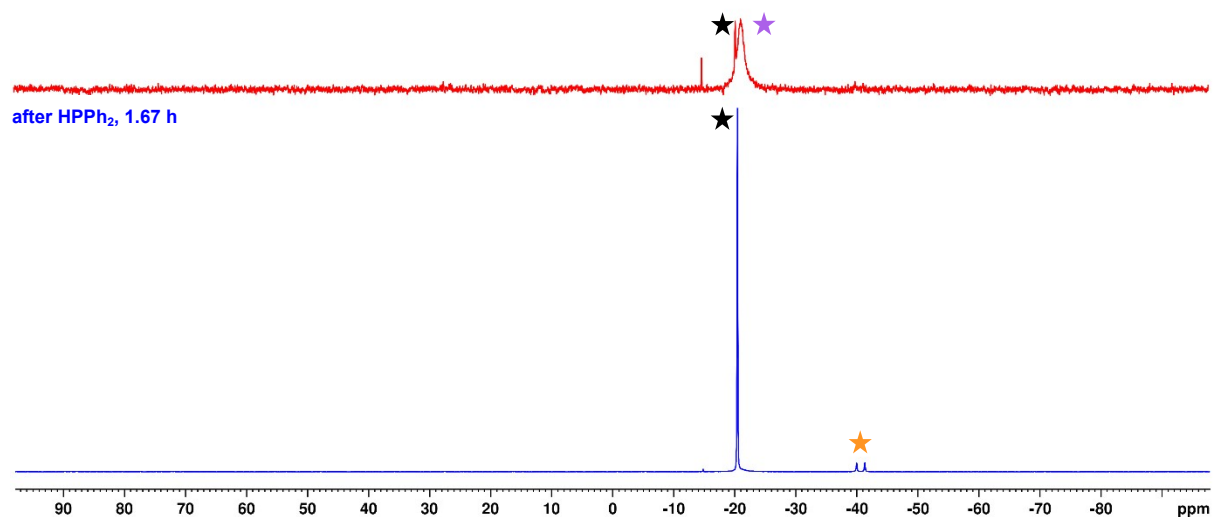


Figure S27 Stacked ³¹P NMR spectra of the catalytic hydrophosphination reaction of 1,1-diphenylethylene by **1** over time. Note a small amount of Ph₂P-PPh₂ (-14.6 ppm). Purple star = catalyst, orange star = HPPH₂, black star = product.

3.3 Hydrophosphination of 1,1-DPE Using $[\text{LiPPh}_2(\text{TMEDA})]_2$

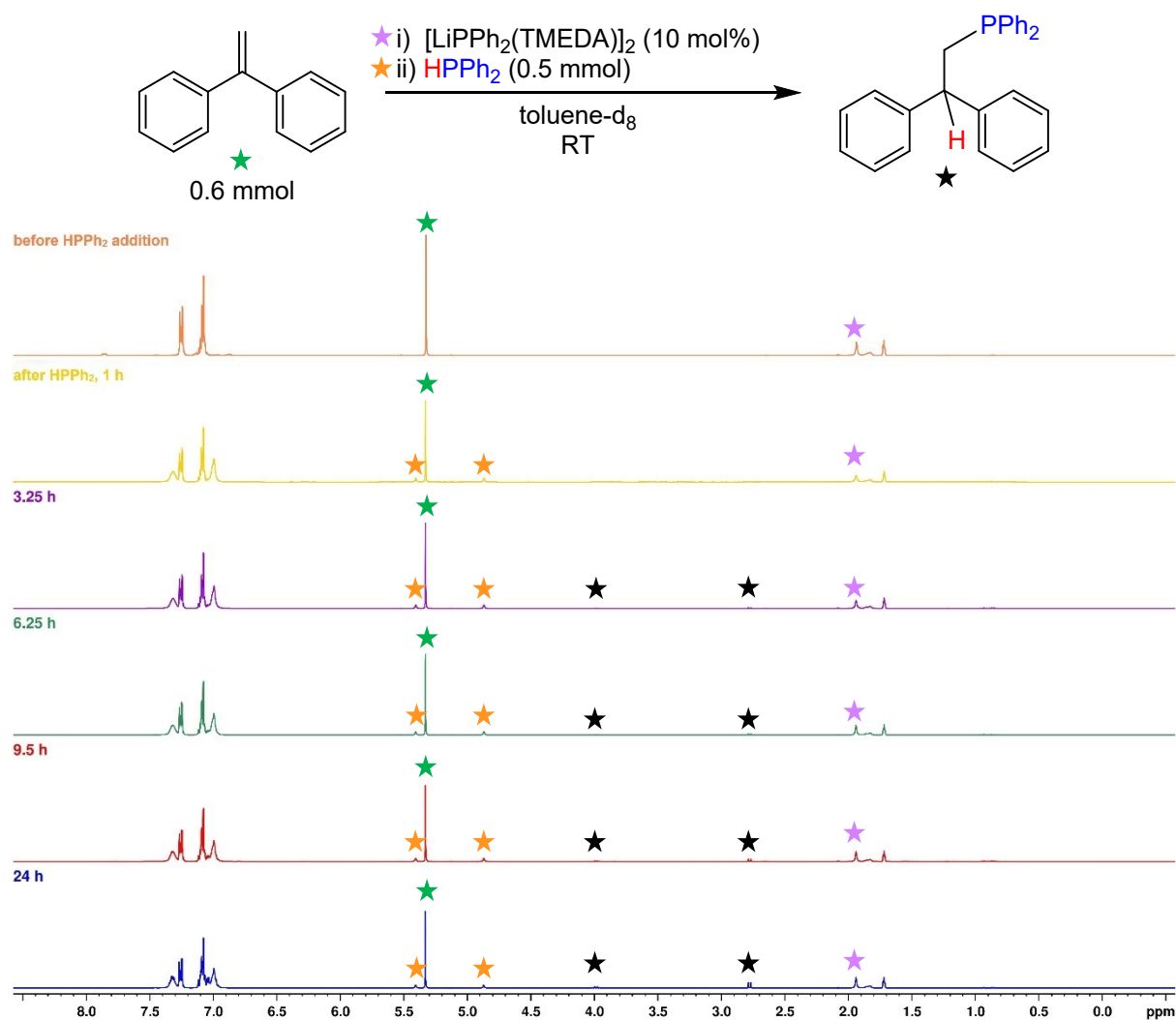


Figure S28 Stacked ^1H NMR spectra of the catalytic hydrophosphination reaction of 1,1-diphenylethylene by $[\text{LiPPh}_2(\text{TMEDA})]_2$ over time. Adamantane (0.044 mmol) was added as internal standard to calculate conversion. Purple star = catalyst, green star = 1,1-diphenylethylene, orange star = HPPh_2 , black star = product.

before HPPh₂ addition

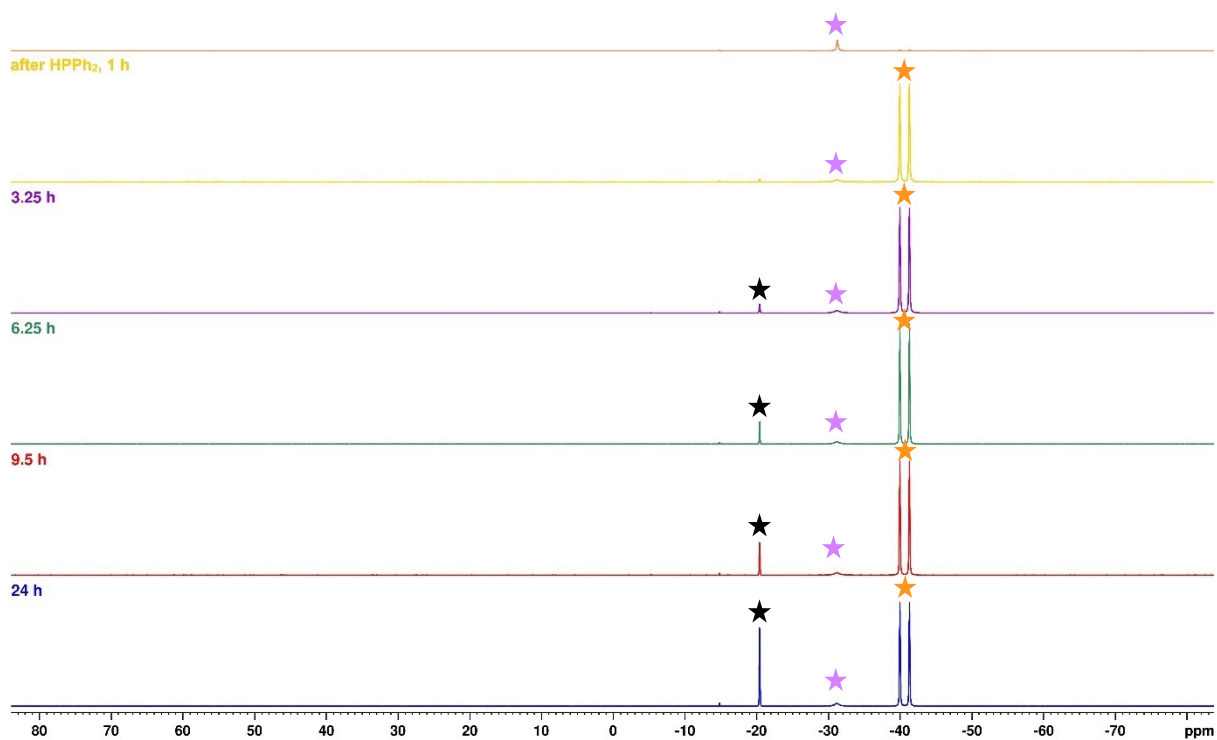


Figure S29 Stacked ³¹P NMR spectra of the catalytic hydrophosphination reaction of 1,1-diphenylethylene by [LiPPh₂(TMEDA)]₂ over time. Note a small amount of Ph₂P-PPh₂ present at -14.6 ppm. Purple star = catalyst, orange star = HPPh₂, black star = product.

3.4 Hydrophosphination of 1,1-DPE Using $[\text{LiPPh}_2(\text{TMEDA})]_2$ and THF

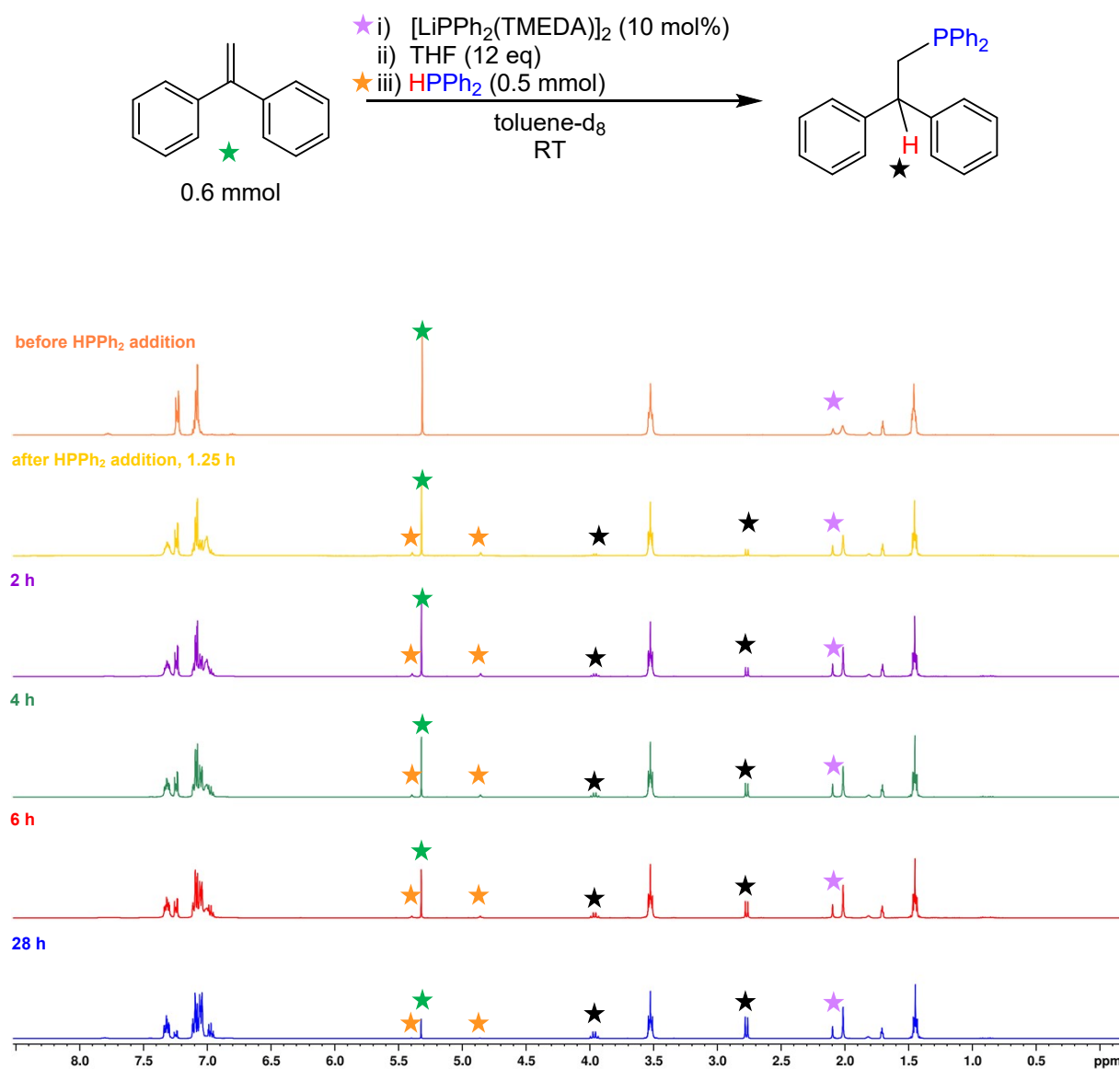


Figure S30 Stacked ^1H NMR spectra of the catalytic hydrophosphination reaction of 1,1-diphenylethylene by $[\text{LiPPh}_2(\text{TMEDA})]_2$ over time. Adamantane (0.049 mmol) was added as internal standard to calculate conversion. Purple star = catalyst, green star = 1,1-diphenylethylene, orange star = HPPH_2 , black star = product.

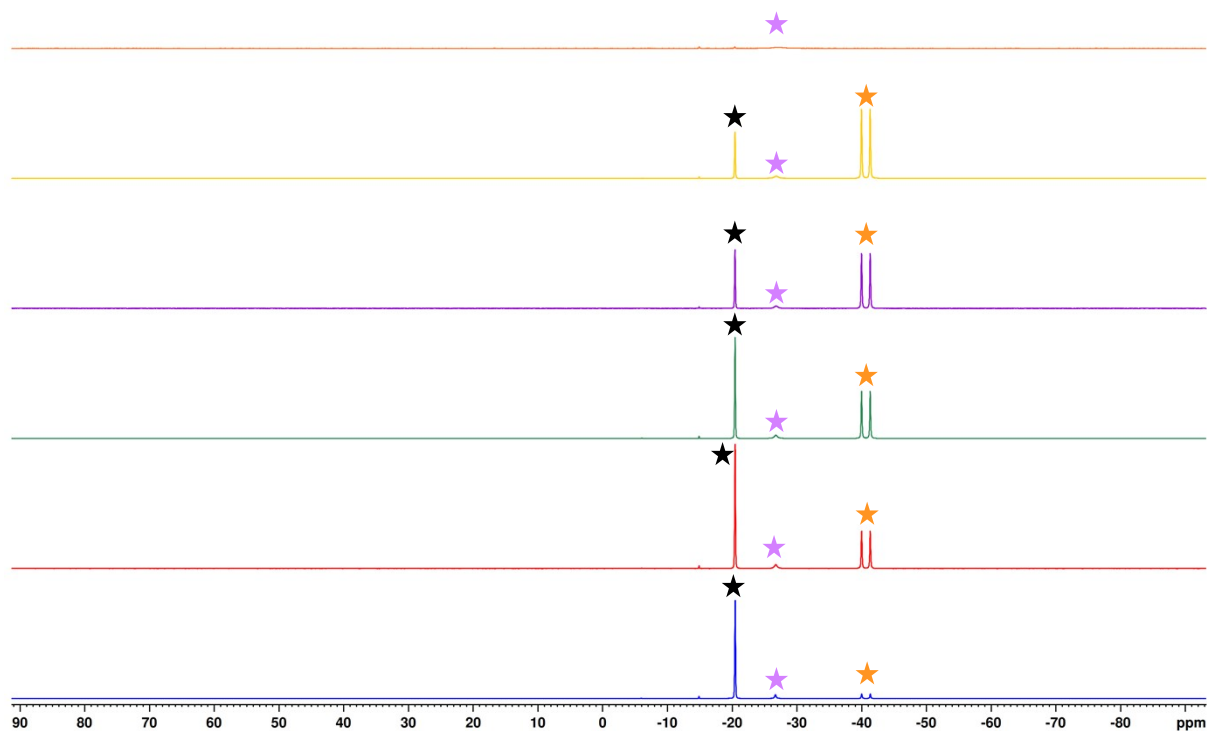
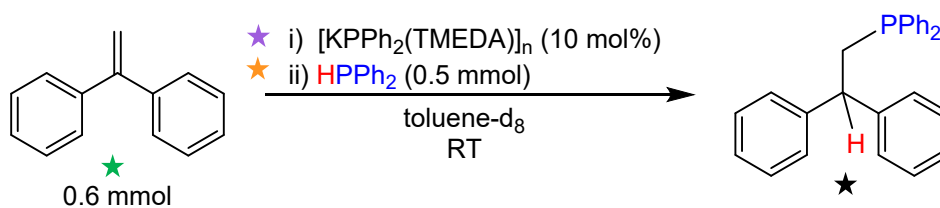


Figure S31 Stacked ^{31}P NMR spectra of the catalytic hydrophosphination reaction of 1,1-diphenylethylene by $[\text{LiPPh}_2(\text{TMEDA})]_2$ over time. Note a small amount of $\text{Ph}_2\text{P-PPh}_2$ present at -14.6 ppm. Purple star = catalyst, orange star = HPPh_2 , black star = product.

3.5 Hydrophosphination of 1,1-DPE Using $[\text{KPPh}_2(\text{TMEDA})]_n$



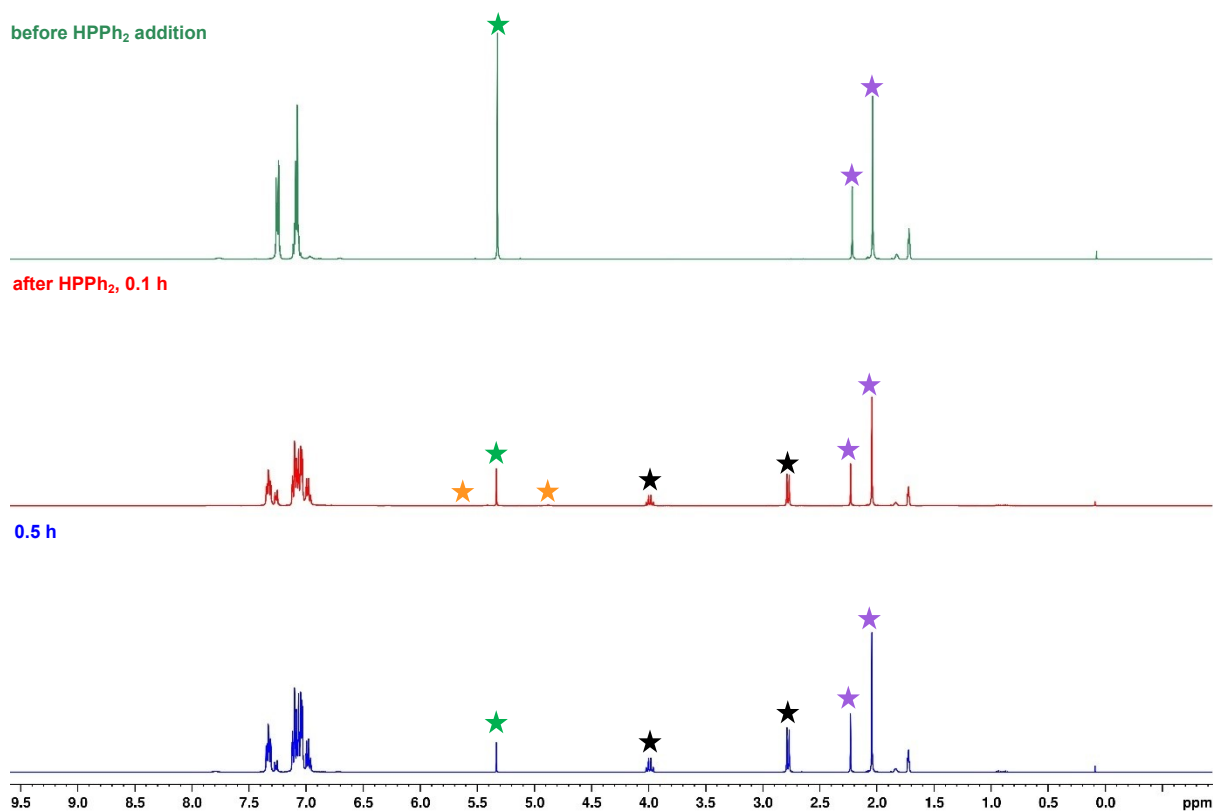


Figure S32 Stacked ^1H NMR spectra of the catalytic hydrophosphination reaction of 1,1-diphenylethylene by $\text{KPPH}_2(\text{TMEDA})$ over time. Adamantane (0.047 mmol) was added as internal standard to calculate conversion. Note small amount of HMDS(H) at 0.1 ppm. Purple star = catalyst, green star = 1,1-diphenylethylene, orange star = HPPH₂, black star = product.

before HPPh₂ addition

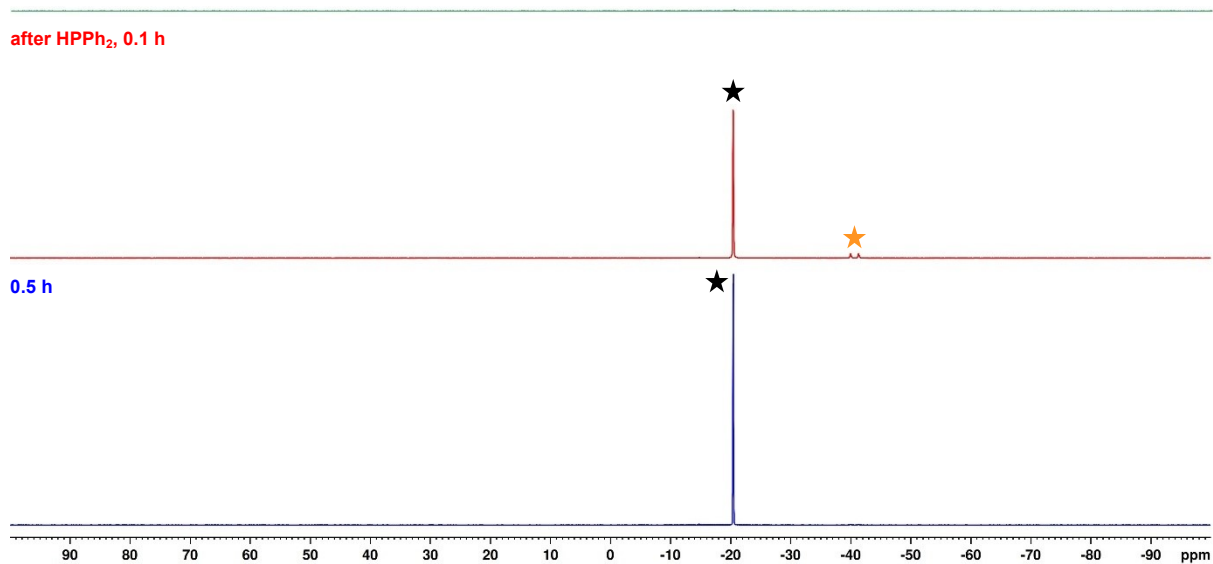
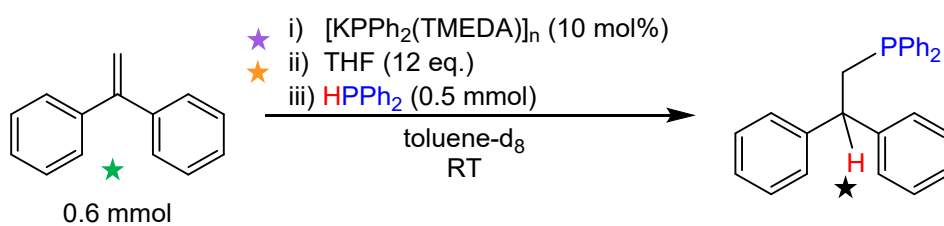


Figure S33 Stacked ³¹P NMR spectra of the catalytic hydrophosphination reaction of 1,1-diphenylethylene by [KPPh₂(TMEDA)]_n over time. Orange star = HPPh₂, black star = product.

3.6 Hydrophosphination of 1,1-DPE Using [KPPh₂(TMEDA)]_n with THF



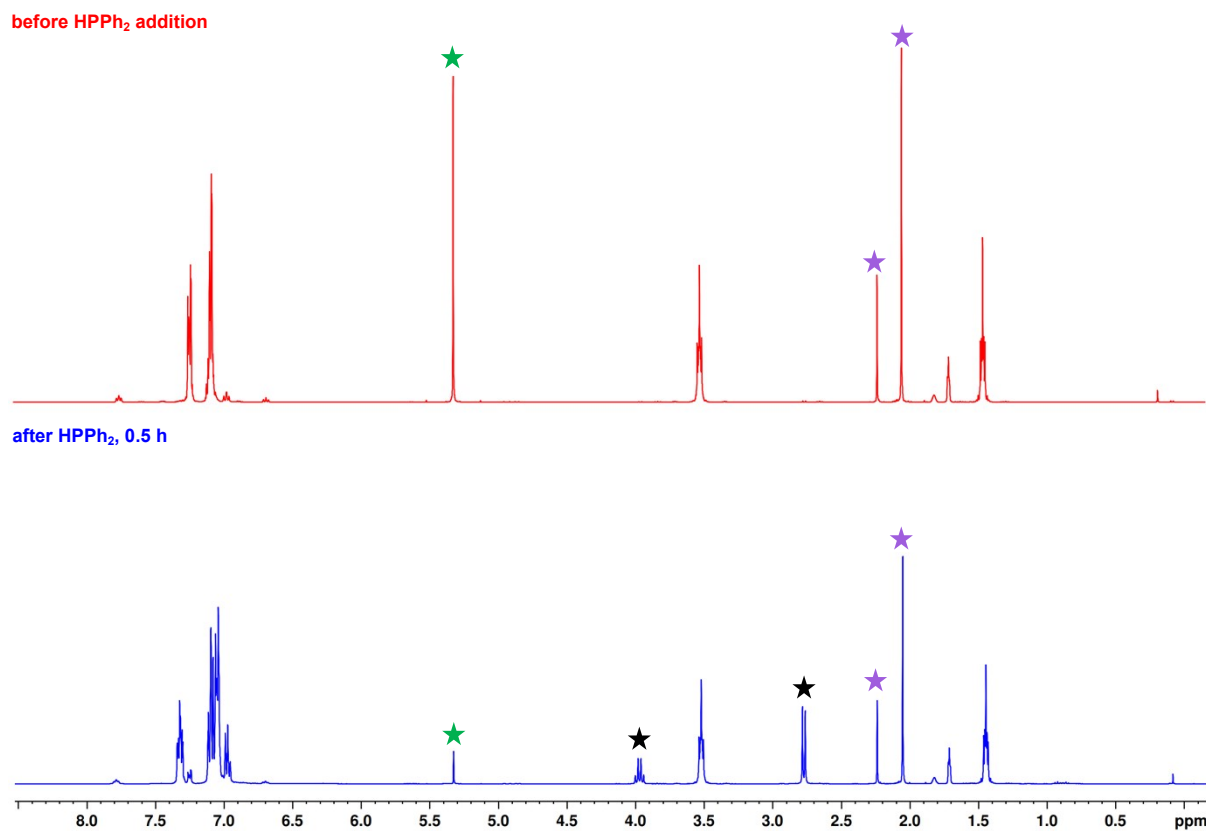


Figure S34 Stacked ¹H NMR spectra of the catalytic hydrophosphination reaction of 1,1-diphenylethylene by KPPH₂(TMEDA) over time. Adamantane (0.041 mmol) was added as internal standard to calculate conversion. Note small amount of HMDS(H) at 0.1 ppm. Purple star = catalyst, green star = 1,1-diphenylethylene, black star = product.

before HPPh₂ addition

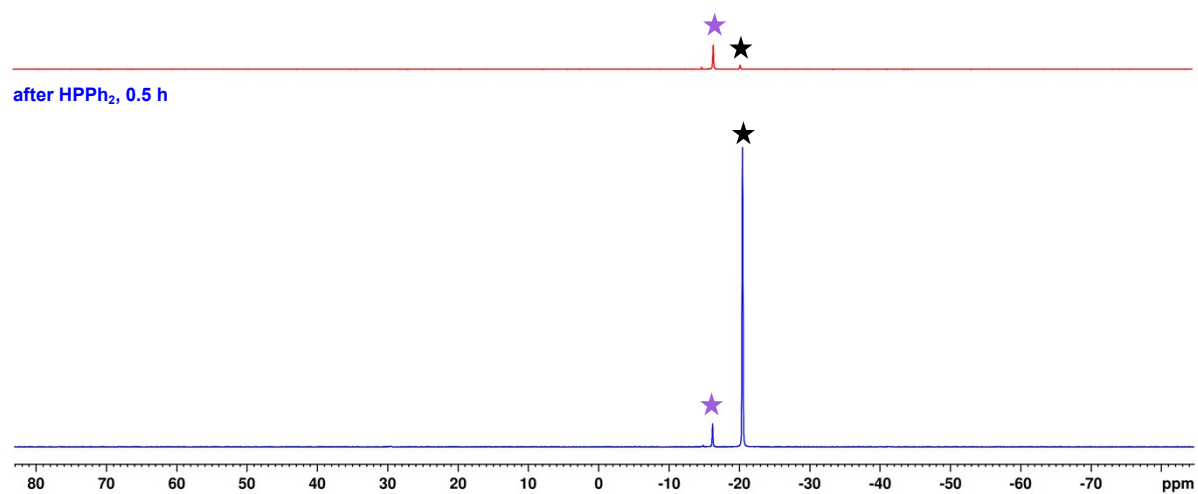


Figure S35 Stacked ³¹P NMR spectra of the catalytic hydrophosphination reaction of 1,1-diphenylethylene by [KPPh₂(TMEDA)]_n over time. Note a small amount of Ph₂P-PPh₂ present at -14.6 ppm. Purple star = catalyst, black star = product.

3.7 Hydrophosphination Dehydrocoupling Control with **1**

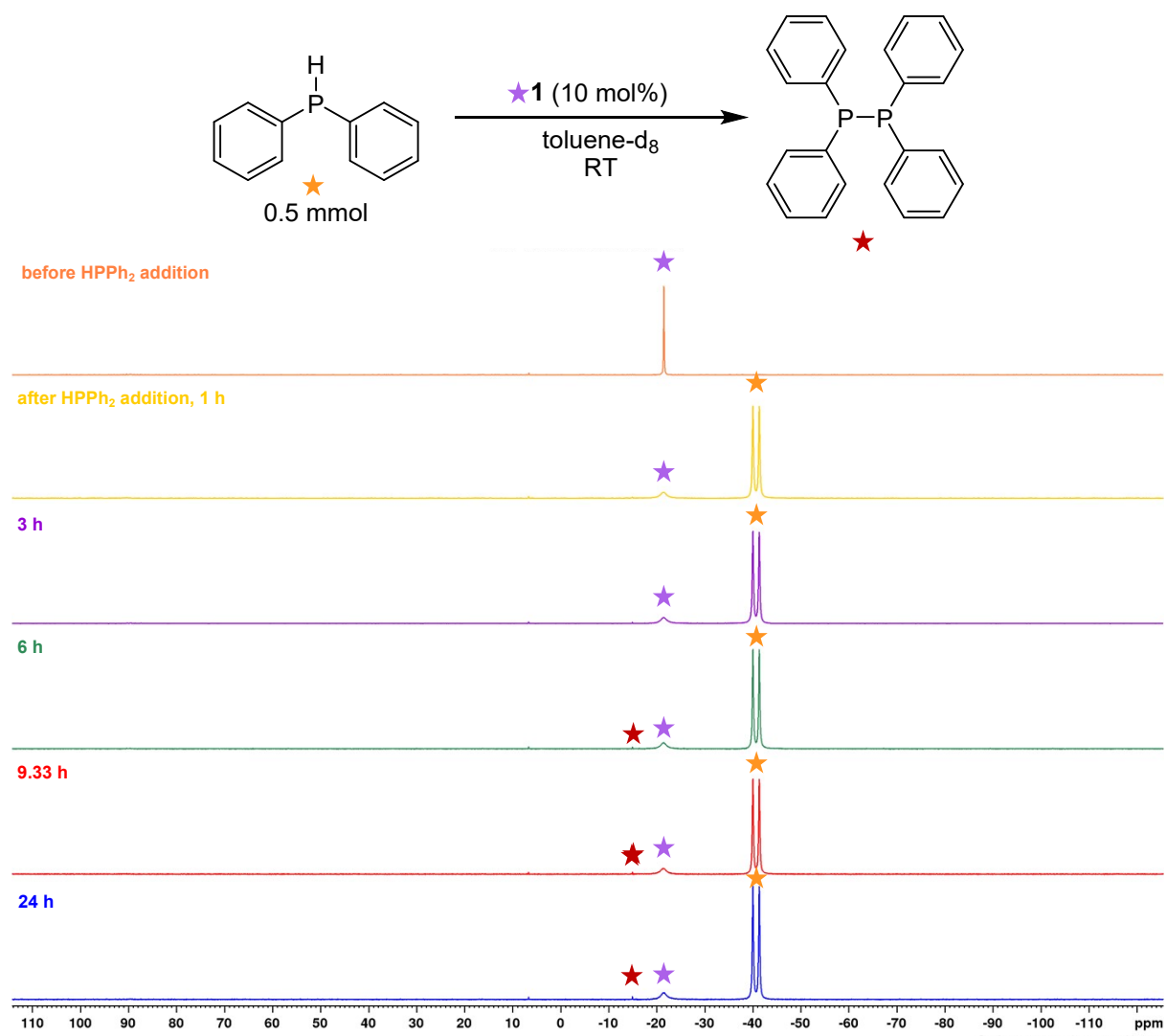


Figure S36 ³¹P NMR stacked plot of the catalytic dehydrocoupling of HPPh₂ over time. Orange star = HPPh₂, purple star = catalyst, red star = Ph₂P-PPh₂. A small amount of PPh₃ is also present.

3.8 Hydrophosphination Excess 1,1-DPE Control with 1

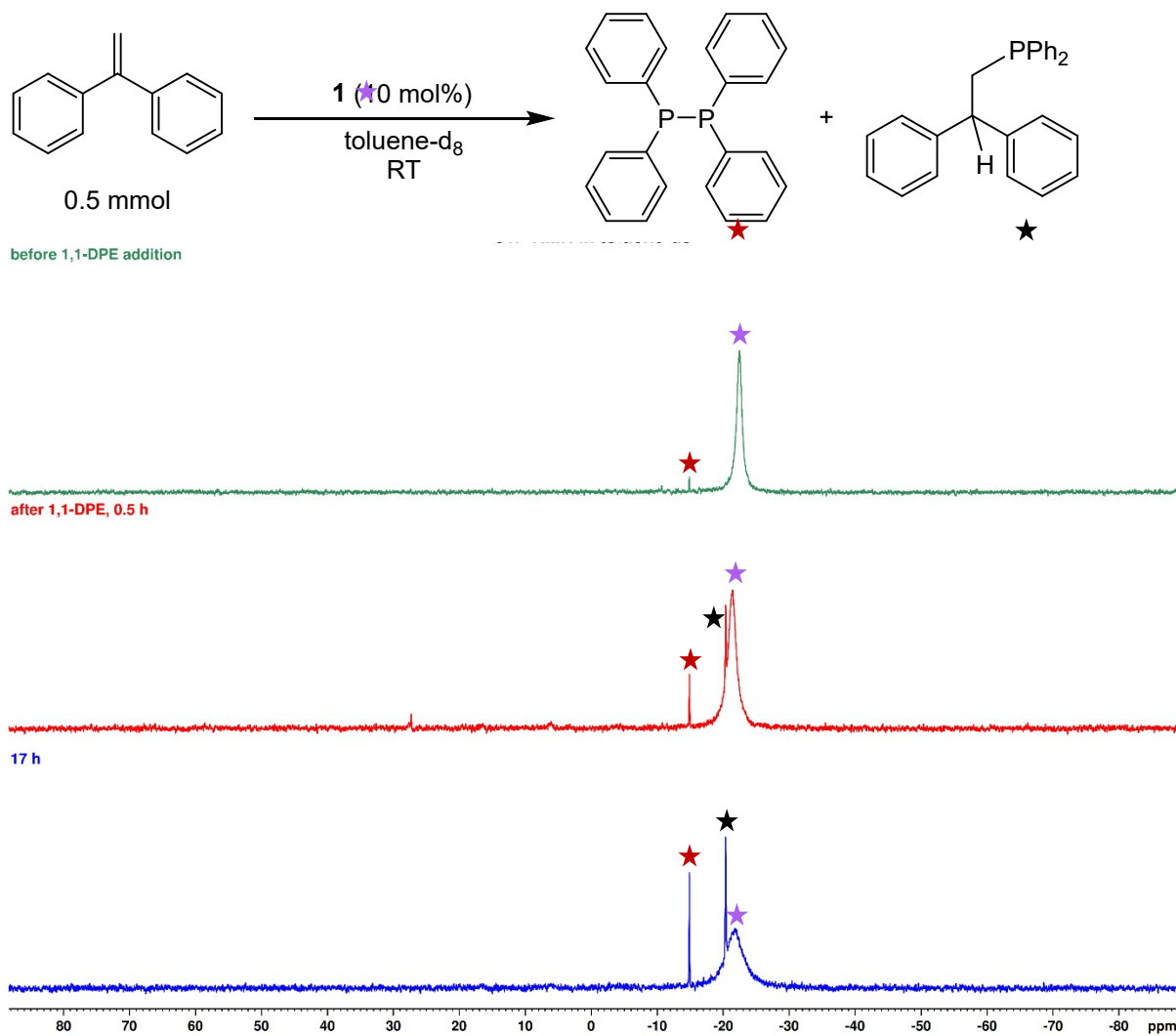


Figure S37 ³¹P NMR spectrum of reaction of 1,1-diphenylethylene with **1**. A small quantity of Ph₂POH (30 ppm) is also present.

4. Computational Details

All quantum chemical calculations were carried out using the Gaussian16 package.¹⁶ The molecular structure optimisations were performed using the M06-2X¹⁷, B3LYP¹⁸ and BP86¹⁹ functionals along with the 6-311+G(d,p) basis set. Each stationary point was identified by a subsequent frequency calculation as minimum (Number of imaginary frequencies NIMAG: 0).

Table S8. Comparison of optimised geometries using different functionals for **LiK.THF**

	XRD	MO62x	B3LYP	BP86
Li-P1	2.6017	2.5586	2.6213	2.6106
Li-P2	2.5993	2.5549	2.6290	2.6251
Li---K	3.8623	3.7570	4.0531	4.0320
K-P1	3.4467	3.2775	3.4057	3.3741
K-P2	3.2418	3.2392	3.3900	3.3773
<i>Average Deviation from XRD</i>		0.073	-0.069	-0.053

BP86 provided the overall best estimate in comparison to the experimental data and therefore was used as the functional throughout the rest of the study. Homometallic compounds $[\text{LiPPh}_2(\text{TMEDA})]_2$ and $[\text{KPPh}_2(\text{TMEDA})]_2$ were also modelled with and without one molecule of coordinated THF in line with the experimental data.

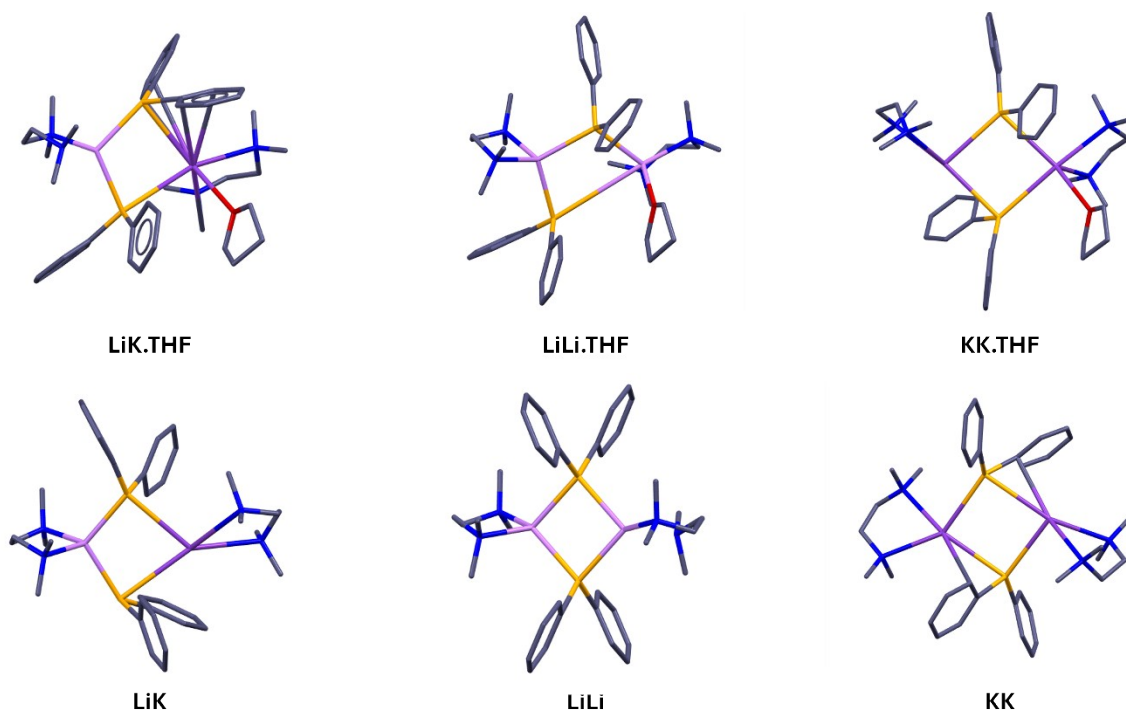


Figure S38. Computed models at the BP86/6-311+G(d,p) level of theory for homo and heterometallic compounds, with and without THF coordination.

4.1 QTAIM Analysis

Quantum Theory of Atoms in Molecules (QTAIM) topological analysis of the electron densities of structures **LiK.THF** were computed with AIMAll professional (version 19.10.12)²⁰ using wavefunction files obtained with Gaussian 16 (C.01) at the BP86/6-311+G(d,p) level. Contour plots were generated in the AIMStudio package.

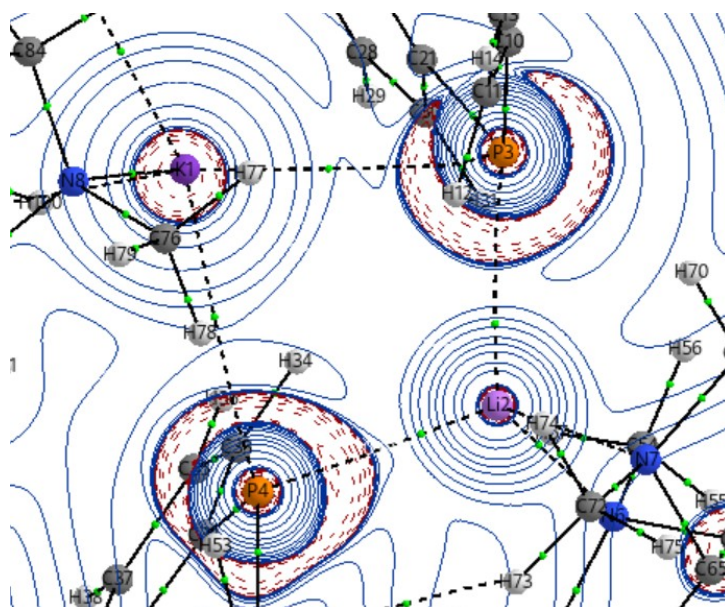


Figure S39. Laplacian ($\nabla^2\rho(r)$) plot of **LiK.THF**
Table S9. BCP and atomic AIM data for **LiK.THF**

	$\rho(r)$	$\nabla^2\rho(r)$	ϵ	$H(r)$
Li2-P4	0.016249	+0.057698	0.096353	0.001036
Li2-P3	0.014847	+0.058696	0.161462	0.001570
K1-P3	0.010882	+0.029865	0.042726	0.000860
K1-P4	0.009869	+0.029266	0.183605	0.001092

4.2 NMR Calculations

Chemical shifts and coupling constants were derived by the GIAO method.^{21–25} ³¹P NMR calculations were performed according to the method outlined by Schulz.²⁶ The calculated absolute shifts of ³¹P nuclei ($\sigma_{\text{calc},X}$) were referenced to the experimental absolute shift of 85 % H_3PO_4 in the gas phase ($\sigma_{\text{ref},1} = 328.35$ ppm),²⁷ using PH_3 ($\sigma_{\text{ref},2} = 594.45$ ppm) as a secondary standard.²⁸ $\delta_{\text{calc},X}$ was determined according to the following formula:

$$\delta_{\text{calc},X} = (\sigma_{\text{ref},1} - \sigma_{\text{ref},2}) - (\sigma_{\text{calc},X} - \sigma_{\text{calc},\text{PH}_3})$$
$$\delta_{\text{calc},X} = \sigma_{\text{calc},\text{PH}_3} - \sigma_{\text{calc},X} - 266.1 \text{ ppm}$$

Following determination of $\delta_{\text{calc},X}$ a correction was applied ($\delta_{\text{calc},X}$). This was determined by creating a calibration curve of experimental vs. calculated ³¹P chemical shifts and applying the correction.

Calculations were performed at the M06L²⁹/6-311g(2d,p) level of theory, on the optimised structures calculated at the BP86/6-311g(2d,p) level. Calculations were performed in the absence of a solvent model, and with THF and toluene solvent models (SMD).

Table S10. Calculated ³¹P NMR shifts for models with non-coordinated THF

	31P calculated values $\delta_{\text{calc,corr}}$			
	Experimental*	Gas phase	THF	Toluene
LiLi	-25.5	-23.6	-24.1	-23.6
LiK	-20.6	-22.7	-23.5	-22.8
KK	-15.7	-15.5	-16.6	-15.7

* Data collected in Tol-d₈ with 0.1mL of THF-H₈

4.3 Reaction Energy Profiles

Energy profiles for the exchange reaction of computed models for **LiLi** and **KK** resulting in formation of **LiK**. The reaction energies were calculated in the gas phase and in both toluene and THF solvent at two different levels of theory. Both indicate equilibrium processes with M062x, which considers dispersion interactions, indicating favourable formation of **LiK**.

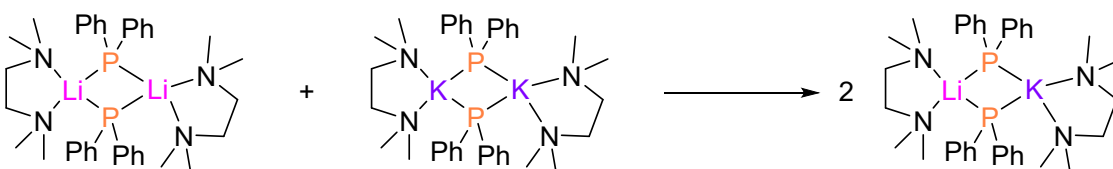


Table S11. Calculated reaction enthalpies and entropies for the formation of **LiK**

	BP86/6-311g(2d,p)		M062x/6-311g(2d,p)	
	ΔH_{rel} (kcal mol ⁻¹)	ΔG_{rel} (kcal mol ⁻¹)	ΔH_{rel} (kcal mol ⁻¹)	ΔG_{rel} (kcal mol ⁻¹)
Gas Phase	-1.07	+1.57	-8.65	-6.54
Toluene	+0.26	+2.90	-6.92	-4.80
THF	+0.05	+2.70	-7.26	-5.15

Table S12. Electronic Energies in Hartrees for BP86/6-311+g(d,p) level of theory

Compound		BP86/6-311+g(d,p)		
		E	H _{corr}	G _{corr}
Gas phase	LiLi	-2320.4369930	-2319.5950530	-2319.7395270
	LiK	-2912.8878621	-2912.0474051	-2912.1971981
	KK	-3505.3369603	-3504.4980463	-3504.6573713
Toluene	LiLi	-2320.4759375	-2319.6339975	-2319.7784715
	KK	-2912.9260373	-2912.0855803	-2912.2353733
	LiK	-3505.3764968	-3504.5375828	-3504.6969078
THF	LiLi	-2320.4785974	-2319.6366574	-2319.7811314
	KK	-2912.9289642	-2912.0885072	-2912.2383002
	LiK	-3505.3793565	-3504.5404425	-3504.6997675

Table S10. Electronic Energies in Hartrees for M062x/6-311+g(d,p) level of theory

Compound		M062x/6-311+g(d,p)		
		E	H _{corr}	G _{corr}
Gas phase	LiLi	-2319.7002414	-2318.8257634	-2318.8257634
	LiK	-2912.0872779	-2911.2145229	-2911.2145229
	KK	-3504.4608143	-3503.5894923	-3503.5894923
Toluene	LiLi	-2319.7372559	-2318.8627779	-2318.8627779
	KK	-2912.1227423	-2911.2499873	-2911.2499873
	LiK	-3504.4974918	-3503.6261698	-3503.6261698
THF	LiLi	-2319.7404749	-2318.8659969	-2318.9990479
	KK	-2912.1264436	-2911.2536886	-2911.3912346
	LiK	-3504.5011283	-3503.6298063	-3503.7752213

5. References

- [1] D. F. Shriver, 'The manipulation of air-sensitive compounds' McGraw-Hill, New York, 1969.
- [2] G. Paolucci, G. Rossetto, P. Zanella and R. D. Fischer, 'Cyclopentadienyluranium(IV) complexes containing phosphido and/or amido ligands: Access to the new complex (C₅H₅)₃UP(C₆H₅)₂' *J. Organomet. Chem.*, 1985, **284**, 213–22.

- [3] P. G. Williard, 'Structure of potassium hexamethyldisilazide toluene solvate' *Acta Crystallogr. C*, 1988, **44**, 270–272.
- [4] M. E. Garner and J. Arnold, 'Reductive Elimination of Diphosphine from a Thorium–NHC–Bis(phosphido) Complex' *Organometallics*, 2017, **36**, 4511–4514.
- [5] J.-Q. Zhang, E. Ikawa, H. Fujino, Y. Naganawa, Y. Nakajima and L.-B. Han, 'Selective C–P(O) Bond Cleavage of Organophosphine Oxides by Sodium' *J. Org. Chem.*, 2020, **85**, 14166–14173.
- [6] M. S. Hill, M. F. Mahon and T. P. Robinson, 'Calcium-centred phosphine oxide reactivity: P–C metathesis, reduction and P–P coupling' *Chem. Commun.*, 2010, **46**, 2498–2500.
- [7] R. Neufeld and D. Stalke, 'Accurate molecular weight determination of small molecules *via* DOSY-NMR by using external calibration curves with normalized diffusion coefficients' *Chem. Sci.*, 2015, **6**, 3354–3364.
- [8] S. Bachmann, B. Gernert and D. Stalke, 'Solution structures of alkali metal cyclopentadienides in THF estimated by ECC-DOSY NMR-spectroscopy (incl. software)' *Chem. Commun.*, 2016, **52**, 12861–12864.
- [9] Agilent (2014). CrysAlis PRO. Agilent Technologies Ltd, Yarnton, Oxfordshire, England. 2014.
- [10] G. M. Sheldrick, 'SHELXT – Integrated space-group and crystal-structure determination' *Acta Cryst. A.*, 2015, **71**, 3–8.
- [11] G. M. Sheldrick, 'Crystal structure refinement with SHELXL' *Acta Cryst. C*, 2015, **71**, 3–8.
- [12] O. V. Dolomanov, L. J. Bourhis, R. J. Gildea, J. a. K. Howard and H. Puschmann, 'OLEX2: a complete structure solution, refinement and analysis program' *J. Appl. Cryst.*, **2009**, 42, 339–341.
- [13] P. Pyykkö and M. Atsumi, Molecular Single-Bond Covalent Radii for Elements 1–118, *Chem. – Eur. J.*, 2009, **15**, 186–197
- [14] A. Bondi, van der Waals Volumes and Radii, *J. Phys. Chem.*, 1964, **68**, 441–451.
- [15] A. Falceto, E. Carmona and S. Alvarez, Electronic and Structural Effects of Low-Hapticity Coordination of Arene Rings to Transition Metals, *Organometallics*, 2014, **33**, 6660–6668.
- [16] Gaussian 16, Revision C.01, M. J. Frisch, G. W. Trucks, H. B. Schlegel, G. E. Scuseria, M. A. Robb, J. R. Cheeseman, G. Scalmani, V. Barone, G. A. Petersson, H. Nakatsuji, X. Li, M. Caricato, A. V. Marenich, J. Bloino, B. G. Janesko, R. Gomperts, B. Mennucci, H. P. Hratchian, J. V. Ortiz, A. F. Izmaylov, J. L. Sonnenberg, Williams, F. Ding, F. Lipparini, F. Egidi, J. Goings, B. Peng, A. Petrone, T. Henderson, D. Ranasinghe, V. G. Zakrzewski, J. Gao, N. Rega, G. Zheng, W. Liang, M. Hada, M. Ehara, K. Toyota, R. Fukuda, J. Hasegawa, M. Ishida, T. Nakajima, Y. Honda, O. Kitao, H. Nakai, T. Vreven, K. Throssell, J. A. Montgomery Jr., J. E. Peralta, F. Ogliaro, M. J. Bearpark, J. J. Heyd, E. N. Brothers, K. N. Kudin, V. N. Staroverov,

- T. A. Keith, R. Kobayashi, J. Normand, K. Raghavachari, A. P. Rendell, J. C. Burant, S. S. Iyengar, J. Tomasi, M. Cossi, J. M. Millam, M. Klene, C. Adamo, R. Cammi, J. W. Ochterski, R. L. Martin, K. Morokuma, O. Farkas, J. B. Foresman and D. J. Fox, Gaussian, Inc., Wallingford CT, 2016.
- [17] Y. Zhao and D. G. Truhlar, *Theor. Chem. Acc.*, 2008, **120**, 215-241.
- [18] A. D. Becke, *J. Chem. Phys.*, 1993, **98**, 5648-52.
- [19] J. P. Perdew, *Phys. Rev. B*, 1986, **33**, 8822–8824.
- [20] AIMAll (Version 19.10.12), T. A. Keith, TK Gristmill Software, Overland Park KS, USA, 2019
- [21] F. London. *J. Phys. le Radium*, 1937, **8**, 397–409.
- [22] R. McWeeny, *Phys. Rev.*, 1962, **126**, 1028–1034.
- [23] R. Ditchfield, *Mol. Phys.*, 1974, **27**, 789–807.
- [24] K. Wolinski, J. F. Hinton, P. Pulay, *J. Am. Chem. Soc.*, 1990, **112**, 8251–8260.
- [25] J. R. Cheeseman, G. W. Trucks, T. A. Keith, M. J. Frisch, *J. Chem. Phys.*, 1996, **104**, 5497–5509.
- [26] P. Felgenhauer, R. Labbow, A. Schulz, A. Villinger., *Inorg. Chem.* 2018, **57**, 15, 9348–9353.
- [27] C. J. Jameson, A. De Dios, A. Keith Jameson, *Chem. Phys. Lett.* 1990, **167**, 575–582.
- [28] C. A. van Wüllen, *Phys. Chem. Chem. Phys.* 2000, **2**, 21372144.
- [29] Y. Zhao, D.G. Truhlar. *J. Chem. Phys.*, 2006, **125**, 194101.